

POLITECNICO DI TORINO

Corso di Laurea Magistrale in Ingegneria Aerospaziale
Specializzazione in Sistemi Propulsivi

Master's Degree Thesis

Build Layout Optimization for Additive Manufacturing of a Turbine Blade



Supervisor
Prof. Daniele Botto

Candidate
Nicola Carbone

Tutor
Ing. Edoardo Peradotto

Anno Accademico 2018/2019

INDEX

Introduction	1
Literature.....	3
I. Additive Manufacturing	4
I.I. Powder bed technology	5
I.I.I. Electron Beam Melting	7
I.I.II. Selective Laser Melting	10
II. Additive Manufacturing process chain	14
II.I. Conceptualization and generation of 3D-CAD model	14
II.II. Conversion of CAD model into AM machine acceptable format	15
II.III. CAD Model preparation	16
II.IV. Machine Setup and job execution.....	19
II.V. Part removal and cleanup	20
II.VI. Post-processing and application	21
III.Design for Additive Manufacturing (DFAM).....	22
III.I. Problem definition or pre-processing	24
III.II. Initial design generation	24
III.III. Design optimization.....	25
III.IV. Design Validation	32
IV. Structural Optimization.....	33
IV.I. Introduction and classification of Structural Optimization	33
IV.II. Topology Optimization	37
IV.II.I. Density Method - SIMP	38
IV.II.II. RAMP Method	42
IV.II.III. Homogenization Method.....	42
IV.III. Shape Optimization	43
IV.IV. Topography Optimization	45
IV.V. Free-Shape Optimization.....	46
IV.VI. Size Optimization	48

IV.VII.	Free-Size Optimization	48
IV.VIII.	Lattice Structure Optimization.....	50
V.	Support structures.....	52
V.I.	AM technologies & Support Structures	53
V.II.	Support Structure Methods in AM	55
V.II.I.	Orientation and overhanging surfaces	58
V.II.II.	Sacrificial or soluble materials as support	60
V.II.III.	Support structures optimization	60
V.II.IV.	Topology optimization for support structures.....	62
VI.	Generation of support optimization method	64
VI.I.	Model geometry & Orientation	66
VI.II.	Thermo-Mechanical distortion model	67
VI.III.	Preliminary support generation (Design Space).....	68
VI.IV.	Topology Optimization	71
VI.V.	FEA Re-analysis and smoothing	77
VI.VI.	Validation of final support designs.....	82
VII.	Conclusions	85
	Appendix (A): L-Shaped geometry.....	87
	Bibliography.....	95

Acronyms

AM	Additive Manufacturing
AMF	Additive Manufacturing File Format
BC	Boundary Conditions
CAD	3D Computer-Aided Design
CNC	Computer Numerical Control (machining)
DED-L	Directed Energy Deposition -Laser
DFAM	Design For Additive Manufacturing
DOE	Design Of Experiment
DMD	Direct Metal Deposition
DMLM	Direct Metal Laser Melting
EBM	Electron Beam Melting
EDM	Electrical Discharge Machining
FEA	Finite Element Analysis
FEM	Finite Element Method
FDM	Fused Deposition Modeling
HIP	Hot Isostatic Pressing
ISE	Isotropic Solid or Empty element
LENS	Laser Engineered Net Shaping
LPD	Laser Powder Deposition
NURBS	Non-Uniform Rational Basis-Splines
OFAT	One Factor At a Time
PBF	Power Bed Fusion
PBF-EB	Power Bed Fusion – Electron Beam
PBF-L	Power Bed Fusion – Laser
RAMP	Rational Approximations of Material Properties
SIMP	Solid Isotropic Microstructure with Penalization
SLA	Stereolithography

SLC	Selective Laser Cladding
SLM	Selective Laser Melting
SLS	Selective Laser Sintering
STL	Standard Triangulation Language
STL	STereoLithography
TO	Topology Optimization
UB	Upper Bound

Introduction

This thesis deals with the study and design of the necessary supports used for Additive Manufacturing processes through a new innovative methodology, which exploits topology optimization in order to reduce the material used, to make supports, and component deformations due to thermal stress and to improve in terms of timing the process execution.

Additive Manufacturing (AM) is a process of building parts by joining material layer by layer from a three-dimensional CAD file, as opposed to subtractive manufacturing techniques (such as turning, milling and so on) [1]. One of the principles of the AM is that the model generated as CAD can be produced bypassing the process planning [2]. Verily, nowadays this last one is still of primary importance and it is one of the main phases of AM (building strategy, orientation etc.), that, carried out as meticulously as possible, guarantees the success of the production of the component and comply with the imposed engineering tolerances. If on one hand the production speed, the lower material consumption, the total freedom of design and the reduction of storage costs are the strong points, on the other hand there is a limited number of materials that can be used, a variable product quality depending on the type of machine used and the skills and knowledge of the operator.



Present Thesis has been developed in collaboration with Avio Aero, a GE Aviation Business that operates in the design and production. It has 4800 people, of which 4200 work in Italy. The head office is in Rivalta di Torino, where there is also the largest production facility. Other important Italian factories are in Brindisi, Pomigliano D'Arco (Naples) and Cameri (Novara) while, abroad, there is a production plant and a test center in Poland. Within the concept of “Brilliant Factory”, or the “Intelligent

Factory”, that is a place of production that can continuously self-improve its products and processes, through the collection, transmission and analysis of data in real time, advanced manufacturing plays a fundamental role and, even more specifically, the additive manufacturing that involves Avio Aero at the forefront thanks to the Cameri plant, one of the largest in the world entirely dedicated to additive manufacturing.

In this regard, together with the Polytechnic of Turin, Avio Aero created the TAL - Turin Additive Laboratory - a joint laboratory created to collaborate on strategic research topics for the aeronautical sector

Literature

This thesis is conceptually divided into three parts.

In the first part the Additive Manufacturing technology is briefly introduced with its advantages and disadvantages, and in particular the powder bed systems and the most used: SLM and EBM. Furthermore, the process chain of the technology under consideration is carried out, from CAD generation to post processing after printing.

In the second, a field that is increasingly taken into consideration for its potential, namely Design for Additive Manufacturing, is introduced, and the methods most used to carry out structural optimizations, from topology to lattice, with their algorithms and their characteristics are described.

In the third part the support structures are analyzed. In particular the additive technologies that need their presence, their purposes and the different structures in circulation with their properties are classified. Special attention is also given to what are the support design variables and how they affect the finished product. Finally, a new advanced methodology for generating support through topological optimization is proposed, by means of an example and an application to an aeronautical component, a turbine blade.

I. Additive Manufacturing

Additive manufacturing became part of Rapid Prototyping around the end of the 1980s.

In fact, the first commercialized system in the world is SLA (Stereolithography), patented by 3D System in 1989, which uses a build platform submerged into a translucent tank filled with liquid photopolymer resin and a single point laser located inside the machine that maps a cross-sectional area (layer) of a design through the bottom of the tank solidifying the material.

Originally exploited to produce prototypes in polymeric materials, nowadays AM is highly competitive with traditional manufacturing techniques, for the production of components also with metallic, composite and ceramic materials, in terms of accuracy, speed and costs (however it depends case by case with still a huge margin of improvement, in the future, from cost and quality stand point). Forms of metal components that cannot be made with conventional techniques (because of complexity of geometry they are usually made by assembling more parts) can be produced with AM technique; optimized parts have been generated, with complex shells, drafting structures and internal channels (provided that the powder trapped inside is then recovered). AM designs may combine what historically were a number of parts requiring joints, assembly, and fasteners into a single functional component.

Thanks to the many advantages that this technology offers, the world of aerospace finds more and more new applications and invests in research to make the latter possible to make them [3]. Manufacturers of AM equipment continue to design, build and sell ever larger and more reliable machines. Precompetitive research continues in universities and corporate research labs, but with in-kind funding from government and industrial partners are becoming widespread. Solid partnerships between machine sellers, software and powders manufacturers and final customers are paving the way for adoption in a wide range of industrial applications and industries.

Given the cost of the machines, most of the work is still carried out by highly qualified engineers in the sector and equipped in the corporate research and development facilities and university laboratories or by service providers able to carry out these initial investments.

This thesis falls within the field of additive manufacturing of metallic materials and components. You can classify the AM techniques based on how the material is made and which energy source is used; however, not all combinations are possible (Fig I.I).



Figure I.I Classification of additive manufacturing techniques.

I.I. Powder bed technology

In general, powder bed fusion technology is the most common metal-based technology used for engineered products, such as aerospace and medical components. A great advantage of PBF techniques is the wide range of CAD software that can be used to generate STL files for these machines. The wide availability of STL (Standard Triangulation Language) file editing software allows fixing, editing, slicing and preparation for 3D printing; powder bed methods offer also the opportunity to build multiple instances of the same part all at once. There are several variations of the powder bed fusion methodology, but substantially all of them share the same principle of work. The two main processes that work with power bed technology are SLM and EBM. The material in the form of powder, of size between tens and hundreds of

microns depending on the technology used (EBM or SLM), is deposited on a plate having as a degree of freedom the translation along the Z axis. A blade or a mechanism of wiper deposits the powder on another plate (also with the same degree of freedom as the previous one but with translation in the opposite direction) part of which will be melted by the laser or electron beam to generate a layer of the component to be made. The space between the surface of the plate or a previously constructed layer and the lower edge of the powder diffusion mechanism characterizes the height of the layer, or rather the thickness. Generally, the last one is of the order of 30-50 microns for the SLM technology and 70-200 for the EBM one. The quality in terms of surface roughness, porosity and microstructure of the layer height is strongly dependent on factors such as beam power (typically adjusted to melt again a certain depth of the previous layer in order to improve adhesion between layers), geometry and speed (lasers or electrons), as well as the size and shape of the powder and the strategy of fusion (Fig. I.II).

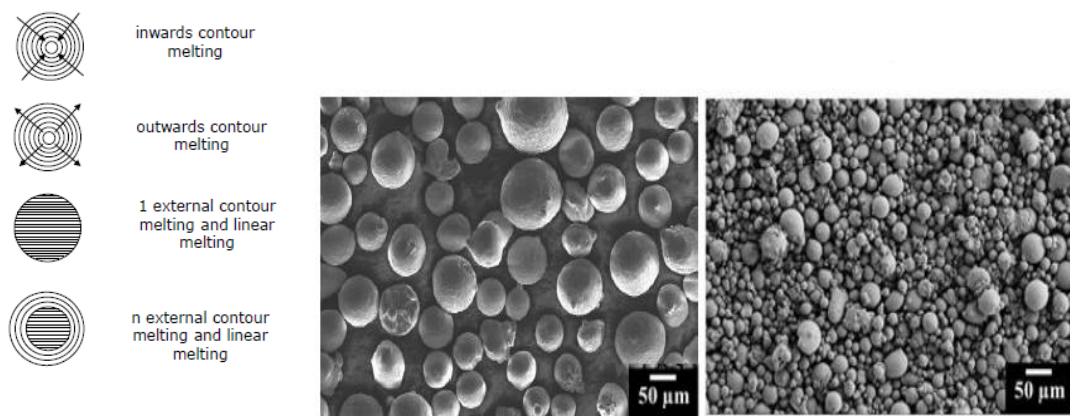


Figure I.II On the left some examples of EBM melting strategy; on the right the dimensions of the powders used for EBM and SLM respectively.

The raster pattern is also a critical factor and it has strong effects on the quality and defect structures of material in the completed part. Once the layer is completed, the platform lowers as much as height of the layer, the powder is redeposited by the wiper system and the process described is repeated.

The optimal combination of the mentioned parameters, which guarantees the desired quality of the product, is not easy to obtain; performing OFAT (One-Factor-At-a-

Time) or DOE (Design Of Experiments) does not preclude the achievement of a perfect synchrony of the variables involved, but it is certainly a right path to follow (Fig. I.III). Anyway, recommended machine parameters are often available from vendors for a subset of well-known materials, but often at additional cost.

Sample	Speed Function	Line Offset	Max Beam Current	Focus Offset
1	low	low	low	-
2	low	low	low	+
3	low	low	high	-
4	low	low	high	+
5	low	high	low	-
6	low	high	low	+
7	low	high	high	-
8	low	high	high	+
9	high	low	low	-
10	high	low	low	+
11	high	low	high	-
12	high	low	high	+
13	high	high	low	-
14	high	high	low	+
15	high	high	high	-
16	high	high	high	+

All these specimens have been grown in one job

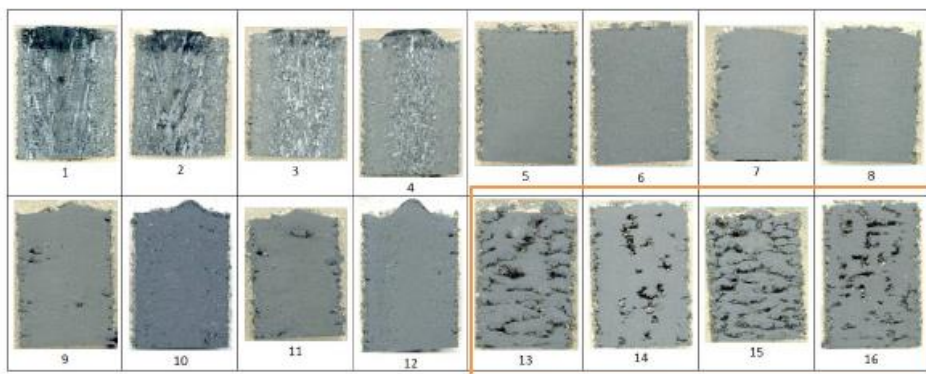
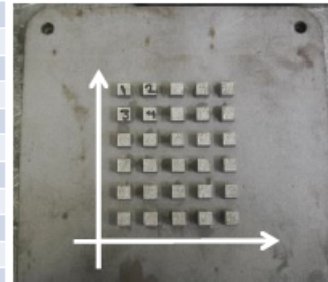


Figure I.III Example of a DOE full factorial for EBM process with four variables (beam speed, line offset, power and focus offset) on two levels (low/high and +/-): $2^4=16$ runs; how they influence internal structure of specimens.

I.I.I. Electron Beam Melting

EBM technology was invented in Sweden in 1993 at the University of Technology in Gothenburg. The Arcam company, founded in 1997, holds the patent for the manufacture of machines for this additive technology. The process is characterized by the focusing of an electron beam on a bed of powder, which metal particles are of the

order of 45-105 microns, in defined areas, causing a temporary melting, then followed by a re-solidification and the consequent formation of the layer. The system is characterized by an electron beam gun, a vacuum chamber (about 4-10 torr), build tank and a powder distribution mechanism. Inside the electron beam gun there is a tungsten filament which, when heated, emits electrons that are then accelerated to a high voltage (about 60 kV) and focused by electromagnetic lenses (Fig. I.IV).

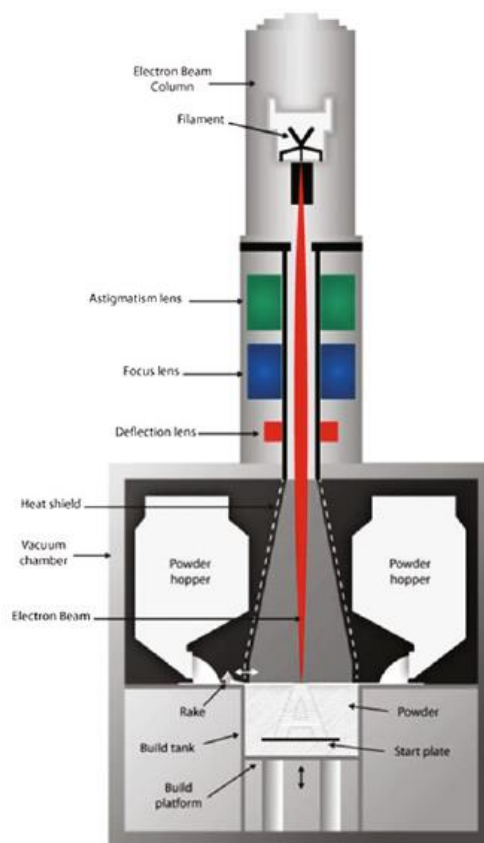


Figure I.IV Detail of the EBM system.

The system just described allows a scanning of the electron beam up to 8000 m/s of speed, an accuracy of the beam positioning of $\pm 0.025\text{ mm}$ and a layer thickness between 0.05 and 0.2 mm [4-6]. The method of production process of the system is essentially the one described in the previous paragraph for a powder bed technology (Fig. I.V). The smallest spot of the focused beam is approximately 100 microns; this allows an accurate construction of the components. Furthermore, more productions can be performed simultaneously in the same work environment.

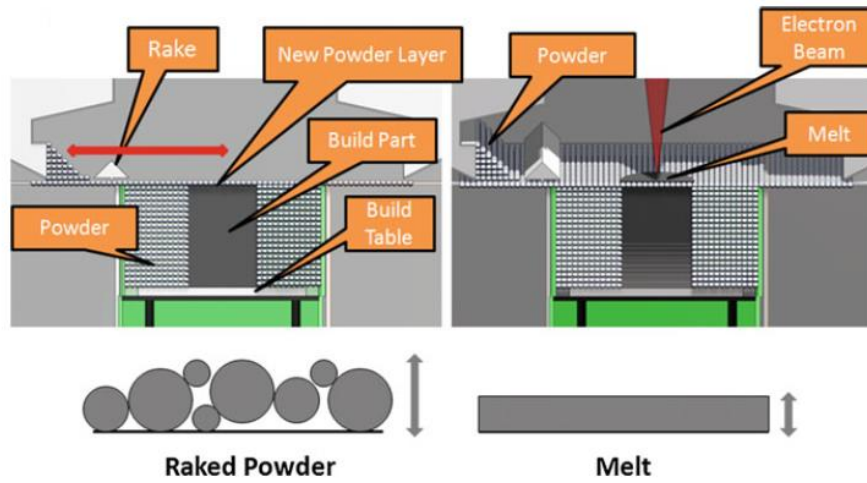


Figure I.V Powder bed methodology of an EBM system.

The building chamber can also be heated up to 680/720 ° C, and it can be kept at a high temperature throughout the production cycle. However, the preheating of the powder varies according to the material taken into consideration; anyway, the reduction of residual stresses, distortions due to cooling (carried out with Elio at the end of production and can last up to tens hours) and the presence of non-equilibrium phases inside of the layers that can cause existence of crack triggers are the main purposes of preheating. Furthermore, a preheating step carried out directly on the powder entails a localized sintering and therefore lower thermal gradients near the edges of the component, and above all a lower need for the presence of supports and greater ease of their removal. The disadvantage of this technique is certainly the minor choice of materials; these must necessarily be conductive. Titanium (and its alloys) is certainly the most used and suitable metal for this technology. In particular, the γ -TiAl and Ti-6Al-4V alloy are increasingly required in the aerospace field [7]. Furthermore, special powders with larger diameter particles and the electrical grounding of the build plate are required due to the electrostatic charge and the repulsion of the finer particles (which are called "smoke") which disturb the layer; consequently, there will be less accurate surface finishes than the laser technique [8].

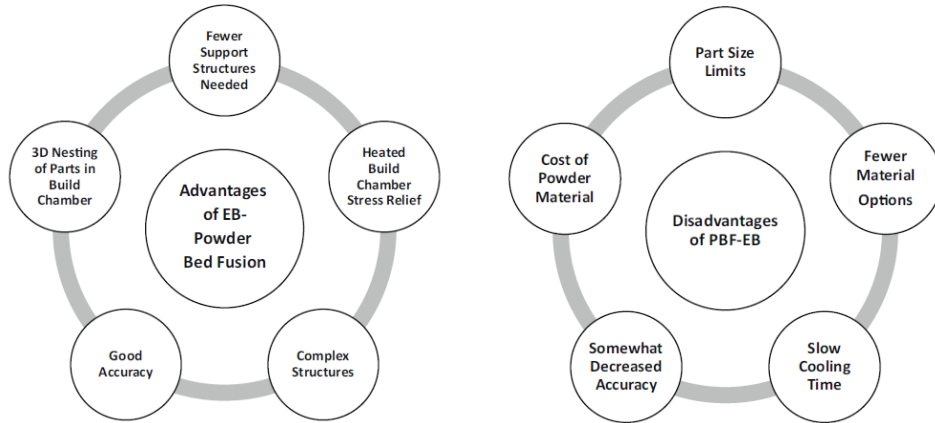


Figure I.VI Advantages (on the left) and disadvantages (on the right) of PBF-EB.

I.I.II. Selective Laser Melting

The selective laser melting (SLM) technique, also defined as a powder bed laser (PBF-L) or direct laser for laser melting (DMLM), was invented in 1993 at the Fraunhofer Institute ILT in Aachen, Germany, thanks to a German research project. The general operating principle of the PBF-L is at times the same as the PBF-EB technology, with the difference that the first one has the laser as its power source and some different boundary conditions (environmental, used materials, etc. that will be described later). Different types of lasers are used, from CO_2 to Yd: YAG, from laser to fiber to disk laser, with powers ranging from 200 to 1000W. The type of laser has a significant influence on the consolidation and fusion of the powders, since the absorption of the materials strongly depends on the wavelength of the laser and on the energy density of the input laser. Furthermore, the laser scanning optics, based on magnetically controlled mirrors that use galvanometers, ensures that the laser beam always cuts perpendicularly onto the powder bed; this technique is more efficient in terms of speed than the DED-L (also known as LENS) one, where the whole system activating the laser beam is moved along the X and Y axes. Despite the fusion and subsequent solidification (with inert gas, to avoid oxidation of the material after build cycle) of the layers occur quickly, that ensures a density at the final superfine component (low presence of porosity), the process strategy has its influence; in fact, as shown in the figure I.VII, when the direction of the beam meets the gas flow, local porosities can

form. EOS adopts the technique where the laser travels in the opposite direction of the gas in order to avoid their interaction.

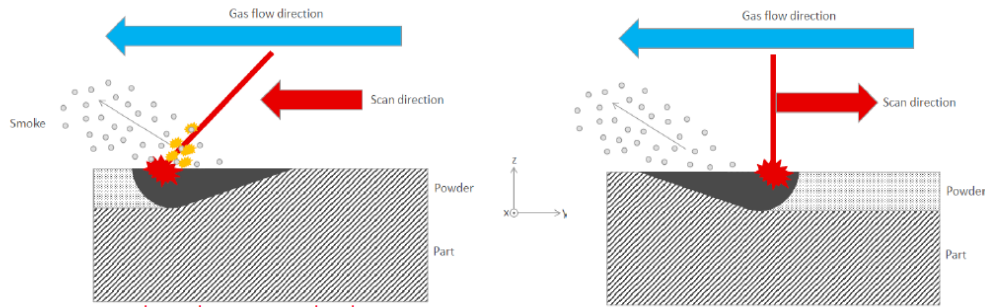


Figure I.VII EOS exposure process in the same gas direction (on the left) and opposite (on the right).

It is of primary importance in the SLM technique to be able to control the size of the pool of fusion, the offset of the scanning line, the speed and power and the thickness of the layer of powder in order to have a complete fusion, or a 100% of density, of a layer itself and a partial / total of the underlying ones (to improve the adhesion between them, Fig. 1.VIII).

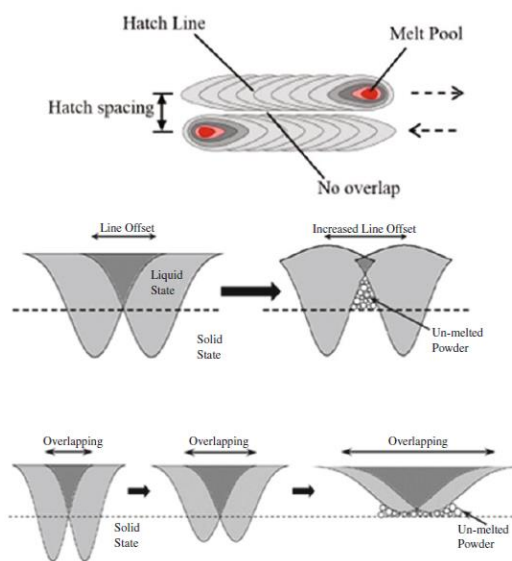


Figure I.VIII Results between different fusion strategies in the SLM technique .

Obviously having a high production speed will always be in conflict having the component of 100% density. Likewise, parameters that influence the final component will be the size of the laser spot, the size of the powder and the orientation of the part. An over spot has certainly the advantage of a faster production, but it is certainly a cause of an inaccurate feature. The powders must be as fine as possible, of the order of 15-45 microns. Finally, the concept of "part orientation" is no less important; in fact, in the pre-planning phase it is necessary to program the presence of supports in very specific points of the part.

At the current state of the art, the materials available and most suitable for this technology are: Aluminum AlSi10Mg, Cobalt Chrome, Maraging Steel, Stainless Steel, Titanium Ti6Al4V and Nickel alloys (Inconel 625 and 718).

In the image below the advantages and disadvantages of this AM technique are summarized.

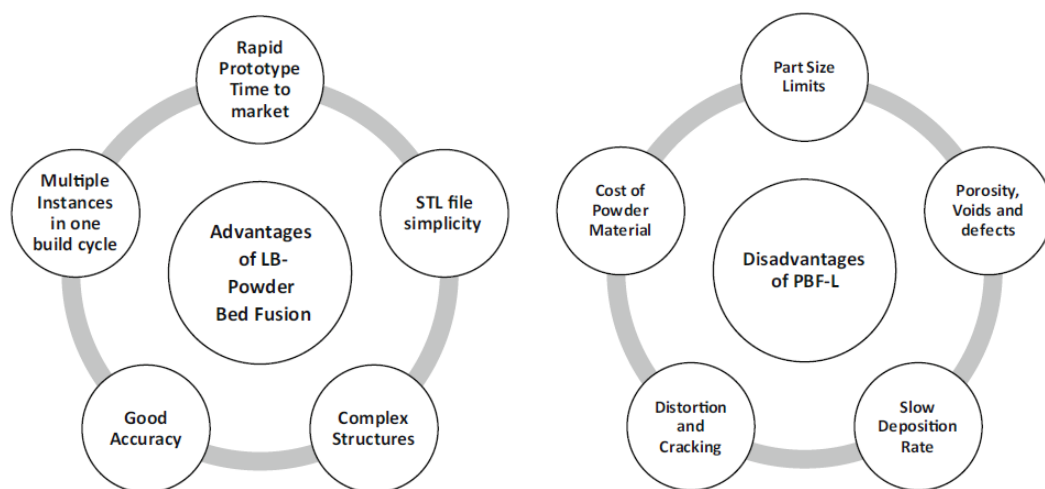


Figure I.IX Advantages (on the left) and disadvantages (on the right) of PBF-L.

To sum up, a comparison can be made between the two most used powder bed technologies in the field of additive manufacturing, remembering that they are not competitors each other; they have different applications depending on the material, geometries, tolerances required, etc.

	PBF-EB	PBF-L
<i>Energy source</i>	Electron Beam	Laser
<i>Power of beam</i>	3-4 kW	200-1000 W
<i>Atmosphere</i>	Vacuum	N ₂ -Ar
<i>Preheating</i>	1000-1100 °C	200 °C
<i>Layer thickness</i>	70-200 µm	30-50 µm
<i>Scanning speed</i>	8000 m/s	3500 m/s
<i>Build rate</i>	60 cm ³ /h	1,8 – 10,8 cm ³ /h
<i>Surface finish [Ra]</i>	~10µ	~4µ
<i>Materials</i>	Only conductive: <ul style="list-style-type: none"> - Ti6Al4V - TiAl - CoCr 	Limited by reflectivity: <ul style="list-style-type: none"> - Inconel 625/718 - Stainless/Maraging Steel - AlSi10Mg - CoCr

Table I.I General technical features compared between the two technologies, EBM and SLM.

II. Additive Manufacturing process chain

In the process chain, required to get the production of the final component, there are some steps to be followed, which, however, may vary depending on the additive technology used. Anyway, we can distinguish six main steps:

- Conceptualization and generation of 3D-CAD model of the design;
- Conversion of CAD model into AM machine acceptable format (STL or AMF);
- CAD model preparation;
- Machine setup and job execution;
- Part removal and cleanup;
- Post-processing.

We could also add a final step that is the application of the component. The process chain is constantly evolving, in fact we could also add an intermediate step, before the construction phase, which is the simulation of the printing process through new advanced software that allow us to obtain reliable results.

II.I. Conceptualization and generation of 3D-CAD model

In each process chain for AM, it starts with the idealization and generation of a 3D-CAD by the expert designer according to the features and characteristics required. Thanks to CAD modeling, the dimensional characteristics of the part are easily memorized and recoverable; therefore, it is necessary to use suitable software such as NX, Solidworks, Catia etc. The solid models are constructed by combining surfaces and giving them thicknesses, according to design requirements. In the past, software had difficulty generating closed solids, so what was apparently closed to the designer was mathematically open; this problem is generally detected in the following step where the CAD file is converted into STL. With modern software, instead, you can generate closed files, or even defined as "water tight". At the end of the modeling, the process chain is apparently one-way that ends with the prototype or the finished component. Indeed, critical feedback can come from subsequent steps such as

incorrect positioning or orientation in the print direction; consequently, a revision and modifications to the project, so to the geometry of component, are necessary. So, AM sometime requires some changes in the product definition in order to make part feasible with this technique, we're talking about Design for Additive, a very important phase of the process, which will be exposed in the following chapters.

II.II. Conversion of CAD model into AM machine acceptable format

Most AM machines use the Stereolithography format, which was the first commercial AM technology from 3D Systems in the 1990s, for reading the input CAD. The STL format captures all the surfaces of the 3D model and performs a triangulation; that is, it approximates a continuous surface in a series of triangular facets of various dimensions which vertices allow the AM process programs to determine the spatial positions of the surfaces of the part in the working space and the surface normal vector associated with the triangle must indicate which side of the triangle is outside vs. inside the part. (Fig. II.I). You can set the minimum size of the triangles, considering that the goal is to ensure that the models created do not have obvious triangles on the surface at the end of the construction. A basic rule of thumb is to ensure that the minimum triangle offset is smaller than the resolution of the AM machine [9].

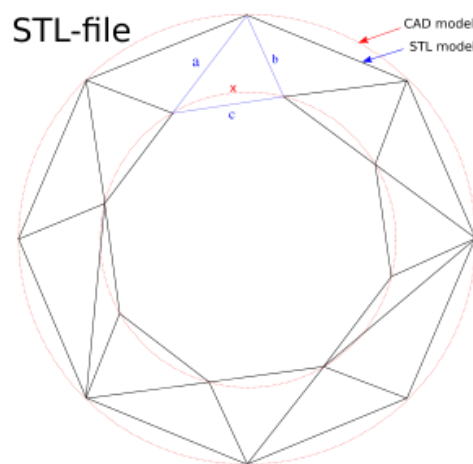


Figure II.I Example of a STL model starting from a CAD model.

Although the translation to the STL format is a necessary and by now consolidated phase of the process, in this conversion step, some information are lost, such as material and size, which can play a critical role in the functionality of the part. The AMF format was developed specifically to prevent these issues, and it contains additional information, omitted by the STL instead; however, the latter continues to be the most widely used format.

II.III. CAD Model preparation

Once the STL file is available, this step can be subdivided into three phases:

- STL file correction;
- Support generation;
- Build file generation.

You need to verify that it is correct and that there are no errors. A complex geometry with many irregular surfaces can cause a non-perfect alignment of the vertices of the triangles, causing gaps in the surface. Other typical errors that can occur after the conversion are the inversion of the triangles normal (the verse of normal is oriented as an internal surface rather than an external one, and vice versa), or missing triangles, double triangles and shells. Some errors are non-critical (such as double triangles) and they can be tolerated. There are software to repair STL files, including MAGICS by Materialise, which is effective when problems occur which prevent the part from being completed. While most errors are detected and corrected by the software, manual intervention by the designer is not excluded.

The presence of the supports is a consequence of the choice of the printing orientation of the part. In addition to minimize the use of supports, a determining factor is the movement of the rake when depositing the powder: during its movement, it can interfere on the newly solidified layer by exerting a force on it. The result will be a deformed or cracked component. The worst case is to have a thin section parallel to the recoater blade [10]. Therefore, it is necessary to place the part on the plate (X-Y

plane) to have the thinner sections inclined at about 5° respect to the recoater (Fig. II.II).

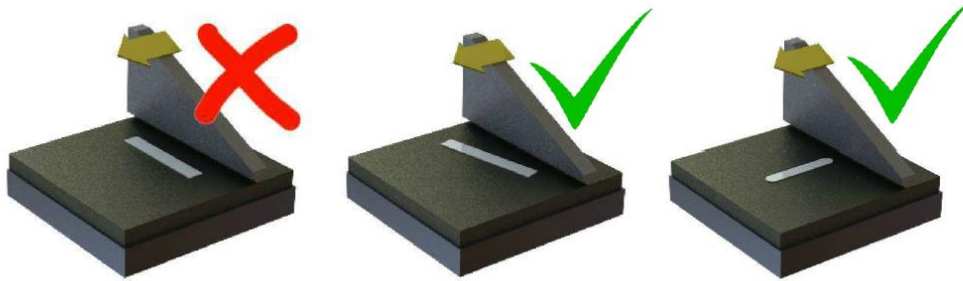


Figure II.II Accepted orientation of a cross section.

For PBF processes, the main role of the supports is to extract heat from the part and to provide a mechanical anchorage to the overhang surfaces to avoid deformations due to thermal stresses during and after build. The supports can be modeled in different ways. As a first approach, they can be generated in the CAD where the part was modeled; alternatively, they can be often generated in the STL file thanks to the previously mentioned MAGICS software. This second approach offers more flexibility in terms of the ability to adapt structures based on needs. However, since the support is not part of the component, but it is material that must then be discarded, it is necessary to optimize them (from the point of view of geometry, volume and positioning) and minimize the consumption of powder. Therefore, careful design of support structure plays a critical role in the success of a build process. Once the STL and CAD with its supports is complete, a slicer program is used to divide the model into layers, based on the chosen printing direction. For a PBF, the thickness of the layer, as we have seen, ranges between 25 and 100 microns. The fundamental parameters for choosing the slice thickness are the beam diameter, rastering strategy, beam power, scanning speed and focus move. Overall, all these parameters determine the amount of energy that affects the powder bed per unit of time. Two algorithms have been performed to carry out slicers: uniform and adaptive slicing. The first is characterized by a slicing with layers of constant thickness, while the second is characterized by a slicing carried out by adapting the thicknesses of the layers to the

sections of the part with high curvature, thus obtaining a better surface finish. Adaptive slicing is difficult to implement for most of the AM system because it does not integrate at best with current machines hardware.

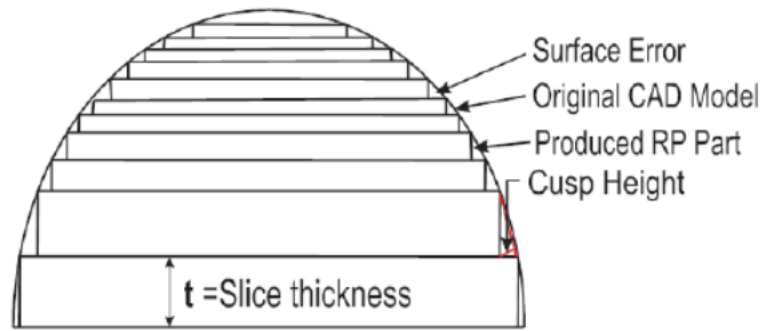


Figure II.III Example of adaptive slicing.

Slicing leads to the classic stair-step effect, which is more accentuated if the thickness of the layer increases and if the inclination of the part increases respect to the printing direction. The best result would therefore be obtained with the part perfectly parallel to the printing direction (Fig II.IV). Surface roughness can be determined only by taking geometric considerations:

$$R_a = \frac{t \cos(\theta)}{4} \quad (II.I)$$

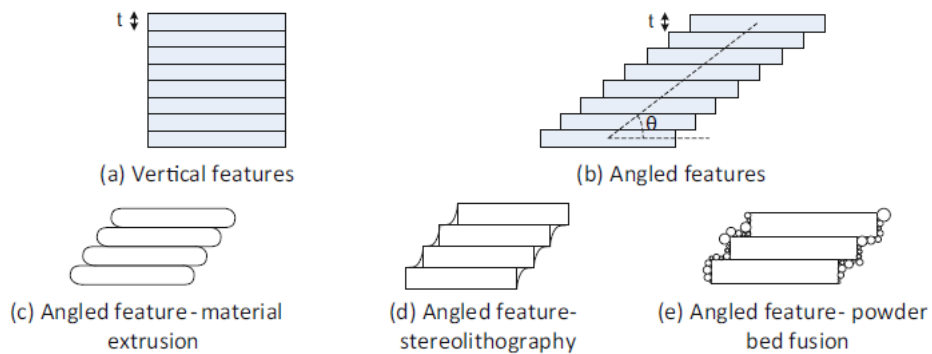


Figure II.IV Stair-step effect and its representations in three different AM technologies.

Once the slice information is generated, it is transferred to the interface program that runs on AM systems.

II.IV. Machine Setup and job execution

The next step is, at this point, the preparation of the AM machine. It consists of two macro phases of activity:

- Machine hardware configuration;
- Process control:
 - A. Build process parameters;
 - B. Material parameters;
 - C. Part parameters.

The hardware setup is characterized by the cleaning of the building chamber from the previous work, loading the new material powder and by the routine checks on controls of the process sensors, such as pressure, flow rate, oxygen etc. The first task of process control is the import and selection of the positioning of the parts in the construction chamber. Then, the manufacturing process parameters, material parameters and part parameters are defined. The manufacturing process parameters define the basic operation of the machine to enable a build environment. Examples of manufacturing process parameters are gas injection, the motion of the powder recoater, ventilation process, etc. Material parameters typically control powder dosing; in fact, a critical parameter is the "dose factor". A "dose factor" equal to 100% means that the plate in the building chamber lowers as much as the plate placed in the dosing chamber rises. Actually, since in the solid phase (after the fusion) the material occupies less volume than the powder phase, the factor must necessarily be higher than 100%. Depending on the needs, the dose factor can vary at any time during the manufacturing process. Another parameter is the oxygen control, which must generally be kept below 1-2% inside the chamber. If the value becomes greater than the one mentioned during the process, the machine stops working; in fact, materials such as aluminum and titanium are reactive and for safety reasons the injection of inert gas continues even after the

end of the additive printing. The part parameters are assigned to the components that must be built. These have already been taken into consideration in the previous step (II.III); therefore, they must coincide exactly with those set during the slicer program. Once the production phase begins, it must be monitored using control systems that release feedback data, including manual ones. An example is the monitoring of the melt-pool, in which a diagnostic beam, coaxial to the beam of the AM machine, monitors the emission intensity of the thermal radiation of the melt-pool and determines its size and spatial distribution of the radiation. If during the build no errors are detected, AM machines will repeat the layering process until the manufacturing is complete. The construction time depends on many factors, first on the height of the component.

II.V. Part removal and cleanup

Once the production of the part is finished, as the process generally does not maintain the high temperatures of the construction platform, the component must be removed immediately. The construction platform is raised, and the not melted powder is removed; the latter will be reused following a sieving to remove unwanted contaminants and particles. Later, being the part and the supports adhered to the plate, the detachment is carried out by means of cutting tools such as band saws or wire electro erosion (EDM, more effective in terms of flexibility).

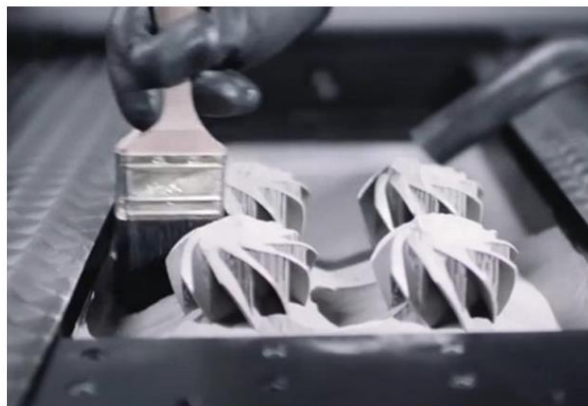


Figure II.V Part extraction after SLM printing.

II.VI. Post-processing and application

The post-processing phase is different depending on the AM technology used and refers to the phases, usually manual, of finishing the parts; in some AM technologies it may not even be done. This last step may include abrasive finishing, like polishing and sandblasting (partially melted powder remains adhered to the part and then removed), or application of coatings. In AM powder bed systems, the post-processing phase requires the removal of the supports from the part as a minimum process. The removal of the supports can be simple and therefore be carried out manually or more complex and then use the CNC tools (which allow to obtain a surface finishing and desired dimensional tolerances). This is a very delicate step, because, due to the high thermal stresses, once the supports are detached from the component, the part tends to deform; therefore, in order to mitigate this risk, it is necessary to carry out a thermal annealing process to relax thermal stresses before the part, together with the supports, is removed from the plate with the EDM technique. The stress relieving is defined as HIP (Hot Isostatic Pressing), where the component is subjected to high temperatures (up to 50% higher than the melting temperature) and to a pressure of about 100-300MPa; the voids inside the part are thus considerably reduced and the density of the material reaches about 95% and in the mean while residual stresses in the component are relaxed (stress relieve) and prevent part from any distortion after support removal.

At the end of post-processing, it should be noted that the characteristics of a component made with the AM technique are different from those of the same component and material but produced with a different manufacturing process (e.g. casting or forging). For example, rapid cooling at the end of the AM process entails a different microstructure than that obtained from conventional production (in general an anisotropic property of the material is always obtained). Consequently, the behavior of the component under different stresses is different to the parts made with conventional processes, even though exactly same material composition; this behavior may be better or worse for an application, and therefore the designer must take this property into consideration during the design phase. That's why material characterization (Metallurgical, Tensile, LCF, HCH etc. mechanical properties) is another crucial aspect of AM techniques.

III. Design for Additive Manufacturing (DFAM)

With additive production, you can take advantage of the possibility of generating particular shapes, such as those obtained through topological optimization, which with conventional techniques could not be carried out, with an acceptable increase in costs. They can also be built directly assembled, avoiding the presence of welds, joints and hinges. The production costs in the world of AM do not therefore depend on the geometric complexity of the products: if at a certain level of complexity conventional techniques must surrender, the AM can instead proceed, defining a region that is defined as "Complexity for free" (Fig. III.I). At the same time, if the request by the components is of small production lots, the AM is certainly a guarantee in terms of economic gains (Fig. III.II).

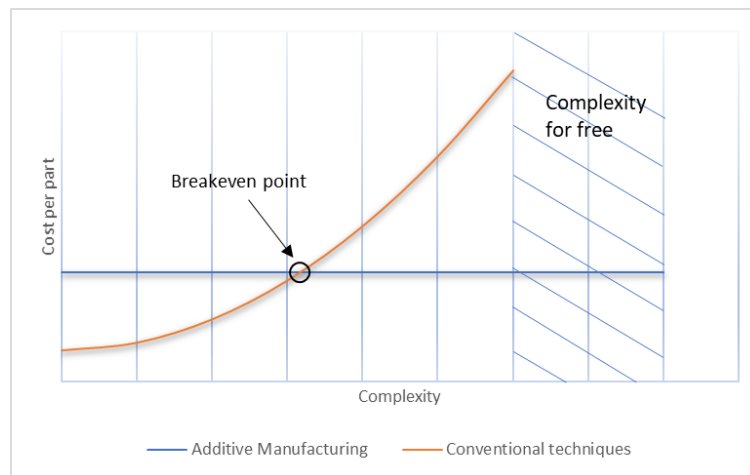


Figure III.I Cost per part as function of its complexity.

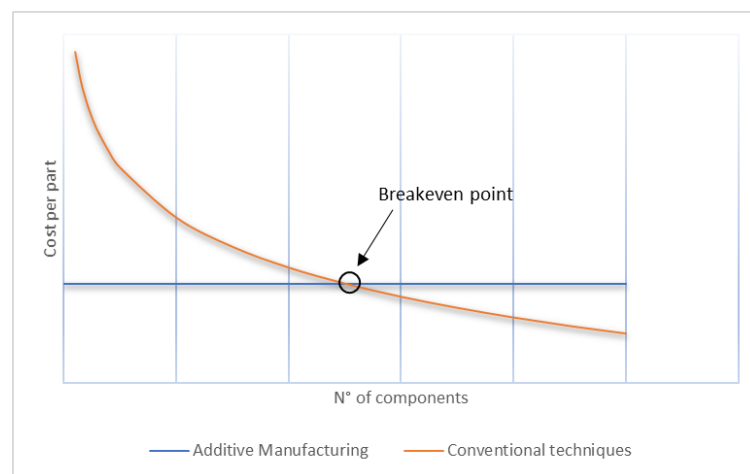


Figure III.II Cost per part as function of number of components to be built.

DFAM has the aim to reduce weight, improve stiffness, mechanical properties, dynamic, static and thermal performance and integrate multiple functions into a single component. It's worth to say, in fact, that the elimination of welding, brazing joints, or do not have more parts assembled together anymore it means also elimination of weakness and failure modes of final part once in service.

The optimization of the component leads to the realization of a product that has the same functionality, or even better, at a reduced weight: which is an advantage in the world of aerospace that is increasingly looking for lightweight components that promise high performance. Furthermore, the saving of material also means less storage and expenses to carry it out.

The guidelines, which will be presented, apply to the part to be built, but in view of the exercise that will be presented in the following chapters, however, they are adapted because they are applied to the support of the component.

Anyway, the path presented is for the redesign and optimization of an existing component. Topological optimization can be divided into four phases:

- Problem definition;
- Initial design generation;
- Design optimization;
- Design validation.

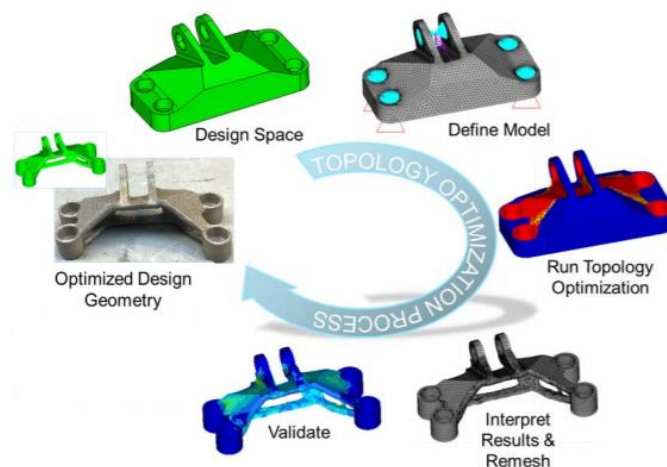


Figure III.III All optimization cycle starting to Design Space definition to validation of new design and printing.

III.I. Problem definition or pre-processing

The definition of the problem is a crucial phase for DFAM and consists in identifying the component object to be optimized, defining the objective function of optimization, understanding the functionality to be monitored and, last but not least, building (or receiving if it is a re-design from an existing component) a solid base model containing information on constraints, loads and working conditions.

This step has been defined as crucial since all that is the output, in the next step it will be input of the initial design and optimization generation phase: for example, an error of consideration on constraints and loads can lead to an incorrect choice of the volumes of design space and non-design space and therefore to a wrong optimization, with consequent extension of the times.

III.II. Initial design generation

In this step the designer must create rough initial shapes, starting with defining functional surfaces. These surfaces generally serve as interfaces between the considered part and its neighbors. Therefore, they must be connected to respect the specified behavior (mechanical load, thermal load ...) [11]. Two particular "structures" are defined:

- *Design space*: It is the volume of the component that can be optimized and therefore can undergo a reduction of material until it reaches the final shape. In designing the Design Space, it may not be careful in detail, so it's important to simplify (if possible) the design space by cancelling features that can be redesigned (e.g. chamfers, internal voids, edge blends etc.) and this in order to give more freedom to the optimization solver. Consequently, the project volume can be extended up to the allowed limits: obviously for allowed limit we mean the interference with another component if the part being optimized is part of an assembly or the eventual form makes assembly difficult. It can be defined by subtracting components assembly volumes of the assembly, functional volumes (e.g. spray cones), machining volumes and tooling path.

- *Non-Design space*: It is the volume in which the optimizer must not act. In the pre-processing the component was analyzed, so all volumes that are not to be modified are marked as any modification compromises the functionality of the component. Non-design space areas can be for example flanges, mechanical coupling areas, fluid-dynamic ducts, bearing seats, oil ducts and so on.

At this step the choice of material is also important. So, the designer must be aware of the AM technique that will be used for the printing of the component that is taken into consideration, because, as already seen in the previous chapters, the choice is not extensive, and every technology has its advantages and disadvantages for certain materials.

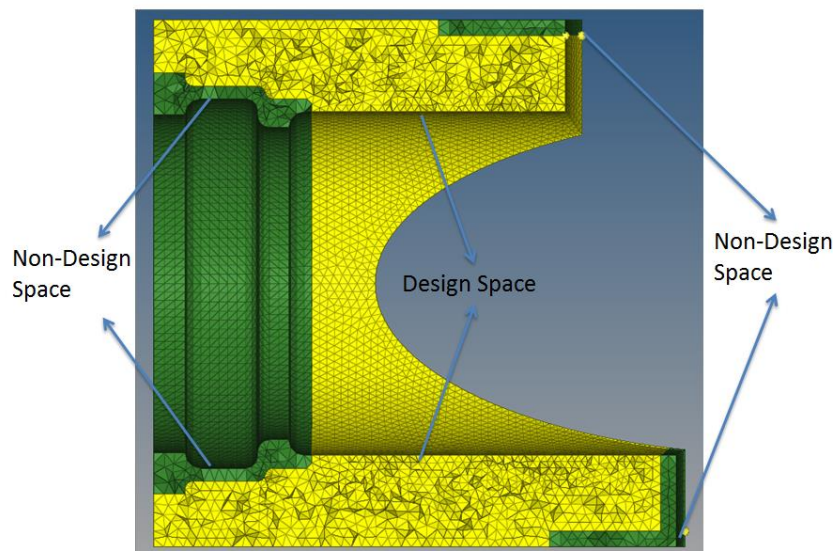


Figure III.IV Example of Design Space and Non-Design Space

III.III. Design optimization

In addition to topological optimization there are also other types of optimization that will be described in the following chapter, and, depending on the imposed objective, one is chosen.

The Optistruct software has been used for this thesis. The software offers several structural responses, as shown in the table (III.I)

Responses can be used individually or in combination with one another to define the constraint functions and the optimization objective.

Mass	Volume	Center of Gravity
Moment of Inertia	Static Compliance	Static Displacement
Natural Frequency	Buckling Factor	Static Stress, Strain, Forces
Static Composite Stress, Strain, Failure Index	Frequency Response Displacement, Velocity, Acceleration	Frequency Response Stress, Strain, Forces
Weighted Compliance	Weighted Frequency	Combined Compliance Index
Function	Temperature	

Table III.I Responses in Optistruct software

Objective functions are any response function of the system to be optimized [12]. Objective functions define constraints on the responses that need to be satisfied once the optimization process has been completed. For example, objective functions can be the minimization or a reduction in percentage of mass, volume fraction, stress, compliance, etc.

In this regard, the exercise proposed in the following chapters is the topological optimization of the supports, and its objective is to minimize the static compliance.

Compliance is the strain energy of the structure and it is calculated using the following relationship:

$$C = \frac{1}{2} \int \boldsymbol{\varepsilon}^T \boldsymbol{\sigma} dV = \frac{1}{2} \mathbf{u}^T \mathbf{F} \quad (\text{III.I})$$

$\mathbf{F} = \mathbf{K}\mathbf{u}$, so:

$$C = \frac{1}{2} \mathbf{u}^T \mathbf{K} \mathbf{u} \quad (\text{III.II})$$

Where:

- C : static compliance.
- \mathbf{F} : forces vector.

- \mathbf{u} : displacements vector.
- \mathbf{K} : stiffness matrix.
- $\boldsymbol{\varepsilon}$: strain vector.
- $\boldsymbol{\sigma}$: stress vector.

For a structure where there are applied displacements \mathbf{u} as subcase, the static compliance C can be considered a direct measure of the stiffness matrix \mathbf{K} , like in (III.II) equation, and it can be written as:

$$C = \frac{1}{2} \mathbf{u}^T \mathbf{K} \mathbf{u} = \frac{1}{2} u^2 K \quad (\text{III.III})$$

Where $\frac{1}{2} u^2$ is constant, and for maximum stiffness, the static compliance C can be maximized.

For a structure with an applied force \mathbf{F} subcase, the compliance can be considered a reciprocal measure of the stiffness, so:

$$C = \frac{1}{2} \mathbf{u}^T \mathbf{F} = \frac{1}{2} \frac{\mathbf{F}^T \mathbf{F}}{\mathbf{K}^T} = \frac{1}{2} \frac{F^2}{K} \quad (\text{III.IV})$$

Where $\frac{1}{2} F^2$ is constant, and for maximum stiffness, the static compliance can be minimized. III.III and III.IV are valid when a single load case or a load step is applied. When the multiple subcases (load steps, load cases) are considered, the weighted compliance is the method used. This response is the weighted sum of the compliance of each individual subcase (load step, load case):

$$C_W = \sum_i W_i C_i = \frac{1}{2} \sum_i W_i \mathbf{u}_i^T \mathbf{F}_i \quad (\text{III.V})$$

This is a global response that is defined for the whole structure. In the case under consideration, we will see that the structural problem is with applied

forces. At this point, optimization is performed. Using algorithms based on mathematical formulations, iteratively the software will provide the optimized geometry. In the next chapter, information on the various structural optimizations with related algorithms will be provided.

Once the optimization process is complete, the new geometry is smoothed. Smoothing is a process to change the position of the vertices of the elements of a mesh in order to improve the quality [13]. In the program used, OSSmooth is a semi-automated design interpretation software, facilitating the recovery of a modified geometry resulting from a structural optimization, for further use in the design process and FEA reanalysis.

OSSmooth for geometry has several uses and can be used to interpret topology or topography optimization results (creating an iso-density boundary surface for the first one or creating beads or swages on the design surface for the second one) and to recover and smooth geometry resulting a shape optimization.

For smoothing, several methods are implemented that can be classified as: geometry-based, optimization-based and physics-based. The two most used are the Laplacian smoothing and Optimization smoothing. The reanalysis process of an optimized component, including smoothing, can be schematized as in the Fig. III.V

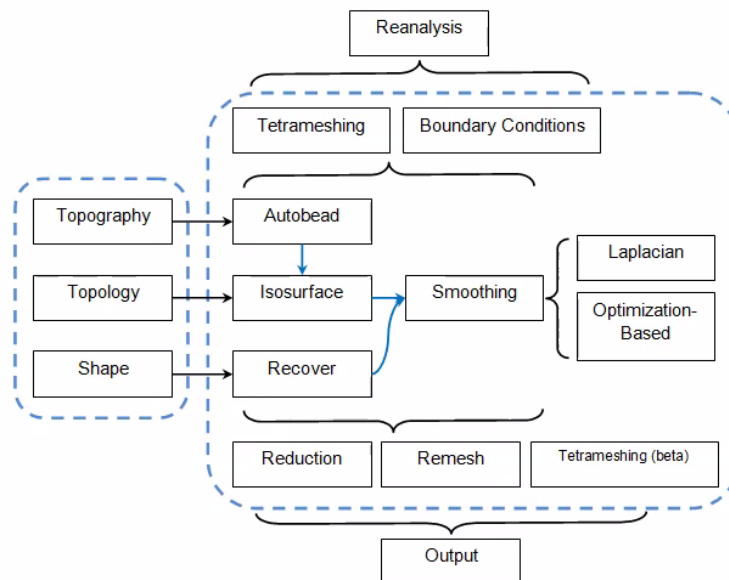


Figure III.V Scheme of the re-analysis process of an optimized component.

Laplacian smoothing is conceptually simpler, but at the same time also very effective, which derives from the approximation of finite differences with the Laplace operator [14]. It morphs and changes the nodal position of the component optimized mesh through transformation:

$$v_i = \frac{1}{V} \sum_{j=1}^N v_j \quad (\text{III.VI})$$

Where v_i is the new position of i -th node, V is the number of adjacent vertices to node i and v_j is the position of the j -th adjacent vertex.

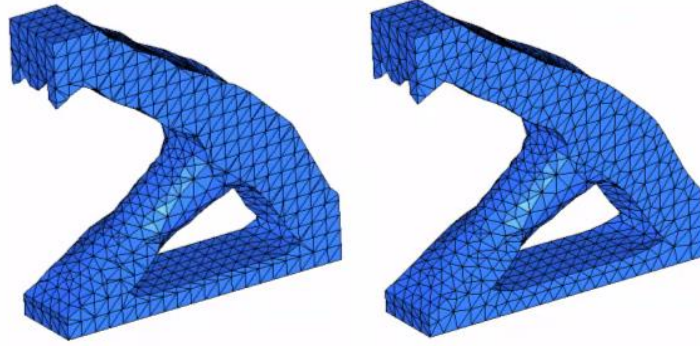


Figure III.VI Iso-surface after topology optimization before (left) and Laplacian smoothing then (right).

As can be seen from Figure III.VI, in the case that a mesh is composed of a rectangular grid (i.e. each internal vertex is connected to four neighbors), then the III.VI operation produces the Laplacian smoothing of the mesh. Sometimes, however, Laplacian Smoothing cannot smooth out more critical surfaces, as can sometimes be the optimized parts. So the software offers an additional smoothing method which is Optimization-based smoothing. In terms of timing and computational costs, it is more expensive than the Laplacian, but it is definitely more effective. While Laplacian Smoothing is based on the morphing of single nodes, Optimization-Based Smoothing aims to minimize the distortion of the elements connected to the single node. This method is based on the improvement of the parameters, quality indexes, of each single element of the mesh, which can be the size, the minimum angle, the skew, the Jacobian

matrix, aspect ratio and so on. Consequently, each quality parameter becomes an objective function and is minimized or maximized according to the need; therefore the optimization acts in compliance with the following equation:

$$f(x) = \min q_i(x) \quad (\text{III.VII})$$

Where:

- $f(x)$: composite function.
- q_i : mesh quality metric.
- x : coordinate where the Opti-smoothing must minimize or maximize q_i .

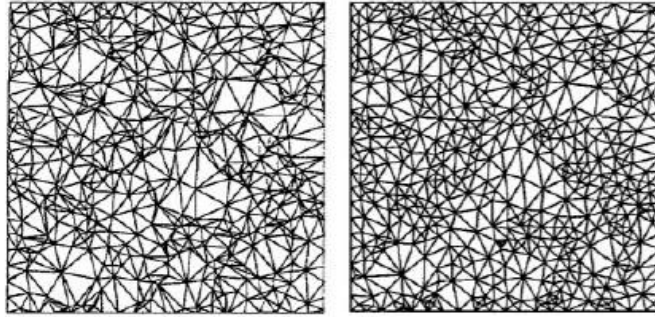


Figure III.VII Mesh before (left) and then (right) the Opti-smoothing process.

As a last step, there is the reconstruction of the optimized part. The optimized and smoothed component is not actually the final geometry, since its surfaces are represented by polygons (deriving from the remesh of the previous phase). This part of the DFAM requires a deep knowledge of the part by the AM designer technique, as it must be able to generate surfaces and volumes that can be printed respecting certain constraints (for example avoiding the generation of hollow volumes).

A method can be simply to set up a CAD modeling software (in this thesis the Siemens NX software was used for CAD modeling) as a background the optimized component and follow the load paths defined by the calculator through simple extrusions, revolutions and trimming (as in Fig III.VIII).

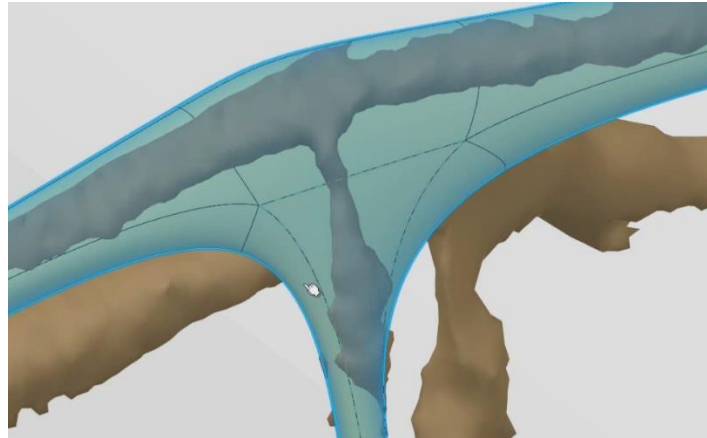


Figure III.VIII Example of a reconstruction of a load path carried out through surface extrusions.

Another method is the construction of NURBS (Non-Uniform Rational Basis-Splines), which generate curves and surfaces enclosed within a polimesh cage; by changing the position of the vertices, faces and edges of the cage, the NURBS changes shape. This approach is more direct, as the optimized geometry is used as a base within which the NURBS will be “pushed and pulled” [15].

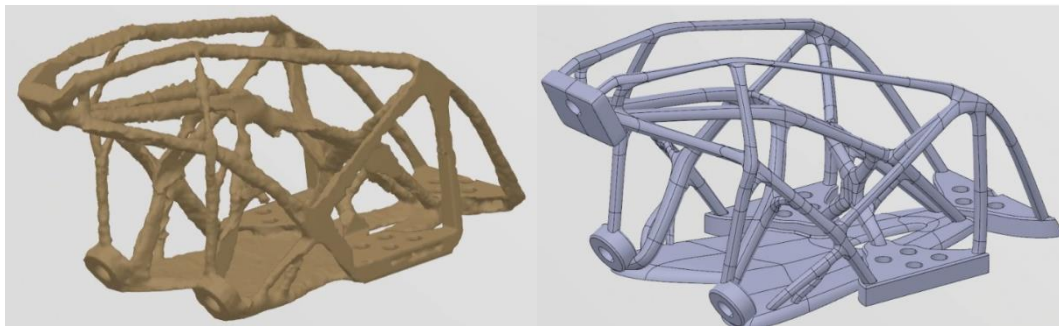


Figure III.IX Example of reconstruction of an optimized component on CATIA.

In the exercise proposed in the thesis, the reconstruction of the optimized support load paths is not mandatory, since only their functionality is important, and this material will be then wasted. It is probable, however, that in some points corrections and adjustments must be made, through CAD modeling, to avoid the failure of the printing process.

III.IV. Design Validation

The last step consists first of all in verifying that the reconstructed component has adequate mechanical properties to overcome the structural analyzes (to compare the results with the pre-existing part) and then validating the producibility of the realized shape and defining the remaining production parameters. Classic structural analyzes are: static, quasi-static, dynamic, HCF, LCF, thermal analysis and so on.

Validity can be obtained either by performing a printing simulation using special software (such as Netfabb, but still not 100% reliable today) or by producing the part directly and conducting a measurement campaign on any component deformations that do not respect the allowable tolerances.

IV. Structural Optimization

In this chapter, a complete description of the structural optimization algorithms will be presented: starting from its philosophy, or rather the concept behind it, ending with the different results that different structural optimizations can bring.

IV.I. Introduction and classification of Structural Optimization

The concept of optimization was born around the first decades of the last century and over time has been able to be taken more and more into consideration, as we have already seen, thanks to the great potential that additive manufacturing offers and to the more and more performance calculators. In fact, in the early years the optimization problems were represented by complex systems with differential equations for which it was not possible to derive the solution in a closed form. With the advent of computers and finite element discretization of the domain, the solution is obtained from systems no more than differential equations but algebraic equations. The optimization process is an iterative process and its basic principle is to obtain the best possible solution for an objective under certain conditions [16].

As written, an optimization problem can be translated into mathematical terms and organized as follows:

- Selection of the *design variables vector* x_i , that depends on the type of optimization being performed:

$$\mathbf{x} = \begin{Bmatrix} x_1 \\ x_2 \\ \cdot \\ \cdot \\ x_n \end{Bmatrix} \text{ which minimizes } \textit{objective function } f(\mathbf{x}) \quad (\text{IV.I})$$

- That is subject to:

$$\begin{cases} g_i(\mathbf{x}) \leq 0, & i = 1, 2, \dots, m \\ h_j(\mathbf{x}) = 0, & j = 1, 2, \dots, n \end{cases} \quad (\text{IV.II})$$

Where $g_i(\mathbf{x})$ and $h_j(\mathbf{x})$ are called *inequality constraint function* and *equality constraint function* respectively and they define the constraints of the optimization problem. So, this kind of problem is defined *constrained optimization problem* [16]. In case you want to maximize the function $f(\mathbf{x})$, just to minimize the negative objective function; so, find x_i which minimize

$$-f(\mathbf{x}) \text{ subject to } \begin{cases} -g_i(\mathbf{x}) \geq 0, & i = 1, 2, \dots, m \\ h_j(\mathbf{x}) = 0, & j = 1, 2, \dots, n \end{cases} \quad (\text{IV.III})$$

So, to formulate a structural optimization we need to describe the variables and the objective function that are at stake and that have already been mentioned:

- *Objective functions*: They are necessary to derive the solution to the problem, and can be linear or non-linear, implicit or explicit. For a structural optimization problem, they can be for example the displacement field, the compliance, and all the elements described in table III.I. A single problem can have one or more objective function, thus having a multicriteria or multiobjective optimization respected.
- *Constraint variables*: As the word itself states, the constraint is a condition that must necessarily be satisfied when the calculator minimizes or maximizes the objective function, and it can also be linear or non-linear. Generally, the constraints can be divided between those that define the admissibility field of the optimization variables and the equality and inequality constraints. Equality constraints are very difficult to manage, and not all optimization problems can reach a solution with these present. Inequality constraints, on the other hand, divide the space of the solution into a feasible zone where all constraints are satisfied and in an unrealizable zone where at least one constraint is not

satisfied. The constraints can be further subdivided into active, inactive, ε -violated and violated. Active constraints bring the equation $g_j(x^*)$ to be null or negative in a design point (x^*); the inactive one bring the same equation to be negative in a design point; the violated one lead to $g_j(x^*) > 0$, while ε -violates are inactive constraints close to being active, i.e. $g_j(x^*) + \varepsilon \geq 0$ with ε very small.

- *Design variables*: They can be continuous or discrete, since they can be defined in an existence field or they can take on a well-defined value, therefore they represent numerical inputs that can change in a well-defined interval; a problem with discrete design variables is called integer programming and it is more complex than using continuous variables.

A simple optimization problem, the objective function can be represented by a continuous curve (supposing a two-dimensional plane), and the (feasible) solution of minimization or maximization is represented by a global minimum or maximum, if in the absence of constraints, and it is called *optimal solution*. It is clear that if, instead, there is one or more constraints, the optimal solution of the problem will no longer be represented by the global minimum or maximum (if it/they don't include it). With the presence of constraint, the space will be divided into two regions: *feasible*, where the constraint is therefore inactive, and *infeasible*, where the constraint is violated.

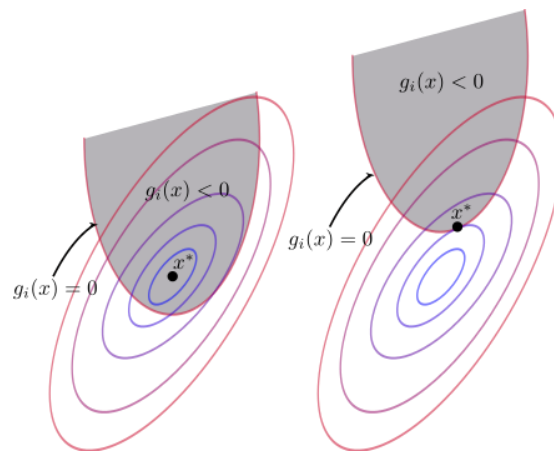


Figure IV.1 KKT (Karush-Kuhn-Tucker) conditions for an optimization problem. With grey color the feasible region, and x^* as global minimum on the left ($g \leq 0$ inactive constraint) and as local minimum on the right.

However, optimization problems are not simply two-dimensional; therefore, to minimize (or maximize) the objective function, it is necessary to carry out an iterative process. That is, starting from a point in the field of existence of the solutions, the direction (S) is obtained which allows to minimize the objective function, in compliance with the constraint conditions.

$$x_i = x_{i-1} + \alpha_i^* S_i \quad (IV.IV)$$

Where x is always the design variables vector, α_i^* is the offset value along S_i that is the searching direction. The iteration process consists initially in the identification of the violated or active constraints (discarding the inactive or ε -violated ones), identification of the S direction, calculation of the α^* coefficient and updating of the optimization variables. If during the iterative process the initially inactive or ε -violated constraints become active or violated, they will take over the iteration.

As the fig.IV.II shows, there are many optimization algorithms. At first glance, in according to Altair guide [17], they can be divided into two macro-sections: once contains the optimizations intended for the *concept-design*, and the other for the *fine-tuning design*.

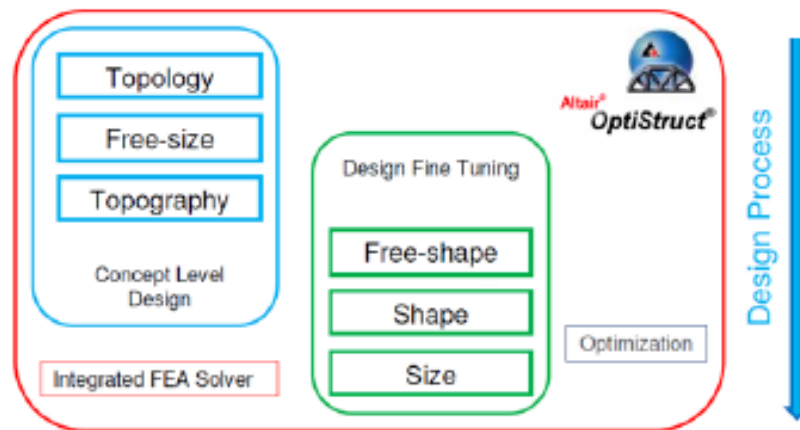


Figure IV.II OptiStruct optimization methods for Concept Level Design and Design Fine Tuning.

Thus, at the early stages of design, the concept design optimization methods are used to get the first forms of the optimized components. Later, if an improvement is needed (in terms of mechanical properties, weight, geometry) of the shape obtained, the fine-tuning design proceeds. In the next paragraphs the different methodologies are analyzed in more detail.

IV.II. Topology Optimization

As we will see in the following chapters, topology optimization is the optimization method used for the present exercise. By "topology" we mean the study of the properties of figures and shapes that do not change when a deformation is performed without "overlapping" or "tearing"[18]. An optimization problem based on this concept is called topology optimization. First introduced by Bendsøe and Sigmund, and extensively treated in [19], it is a mathematical technique that generates a shape and a distribution of material and voids optimized for a structure within a well-defined space, which was mentioned in the previous chapter and is called design space or *ground structure*. By assigning a valid project and an analysis with the appropriate boundary conditions BC, loads and constraints, the software predicts the shape and optimal distribution of material and voids for the application, performing an iterative process.

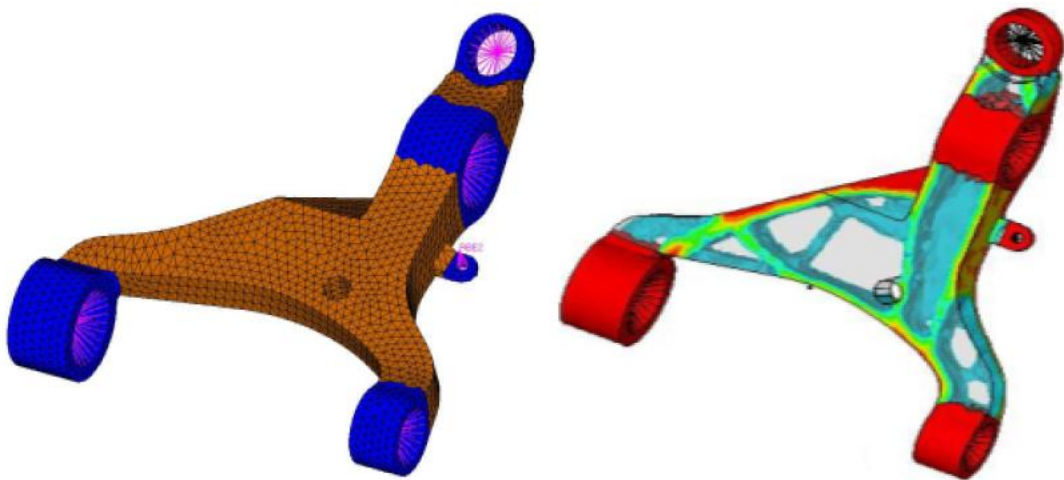


Figure IV.III Control Arm Topology Optimization.

In the topology optimization problem, expressing the stiffness tensor as a value that depends continuously on the density of the material, the density will then be a design variable.

$$E(\rho_i) = \rho_i^p E_0 \quad (\text{IV.V})$$

Where $p > 1$ is the *penalty factor*, ρ is the material density and:

$$\begin{cases} E(\rho = 1) = E_0 \\ E(\rho = 0) = 0 \end{cases} \quad (\text{IV.VI})$$

The density is assigned to each element of the mesh and oscillates between 0 (void) and 1 (solid). This result is also called *0-1 problem* or ISE topology (Isotropic Solid or Empty elements), where an element exists or not. Using a continuous function to define the density in the defined interval $[0,1]$, not only simplifies the problem, but also makes it possible to generate elements with intermediate values as well as 0 and 1; however, elements with 50% density are not physically reasonable. Indeed, the substantial difference between the different topological optimization algorithms lies precisely in how they handle the interpolation of the intermediate density values in this interval. There are several methods using different bases for the assignment of density to the elements, but the two mains are the *density method* (SIMP) and the *homogenization method*.

IV.II.I. Density Method - SIMP

The Solid Isotropic Microstructure with Penalization (SIMP)-model, also known as the *penalized, proportional stiffness model*, is a gradient-based model [20] expressed in mathematical terms as presented in equation IV.V. The SIMP algorithm starts from a uniform distribution of density in the elements of the design domain and a volume fraction equal to the specified one. The first step in the iterative analysis is the resolution of equilibrium equations, then it is followed by a sensitivity analysis that calculates the derivatives of design variables (density of elements). To ensure numerical stability, filtering techniques are applied before the densities are updated. This procedure is repeated until convergence is reached.

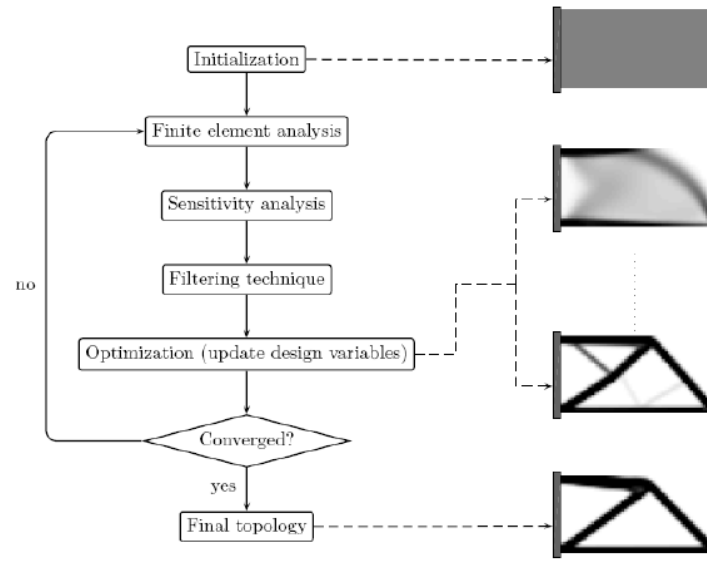


Figure IV.IV Work scheme of SIMP algorithm for topology optimization.

By choosing p greater than one, the presence of elements with intermediate density values that contribute to the total stiffness is avoided.

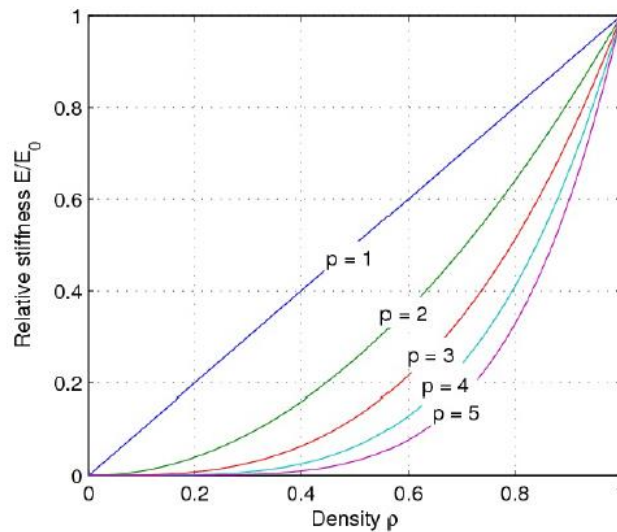


Figure IV.V Relative stiffness in function of density, varying penalty factor.

SIMP interpolation can be expressed:

$$\frac{E}{E_0} = k(\rho) = k_{\min} + (k_{\max} - k_{\min})\rho^p \quad (\text{IV.VII})$$

Acceptable values of the parameter p are between 2 and 5. Assuming a high number leads to a solution surely closer to the classic ISE ("black or white"), however, we will obtain lighter but infeasible geometries that present the phenomenon of checkerboarding: in fact, the solver brings "checkerboard" configurations in which full and empty elements alternate. Thus, the result is a structure with spurious stiffness and no physical meaning.

To overcome this problem there is a further parameter that is called *sensitivity filter* r . The filter works by mediating, at each iteration, the density of each element with those of neighboring elements within a radius of action of r times the average size of the element. In this way the solver forces the final configuration to create beams structures with a diameter equal to $2r$ times the average dimension of the elements [26]. In the figure IV.V you can see, in 2D, the effects of the two parameters in the final optimization.

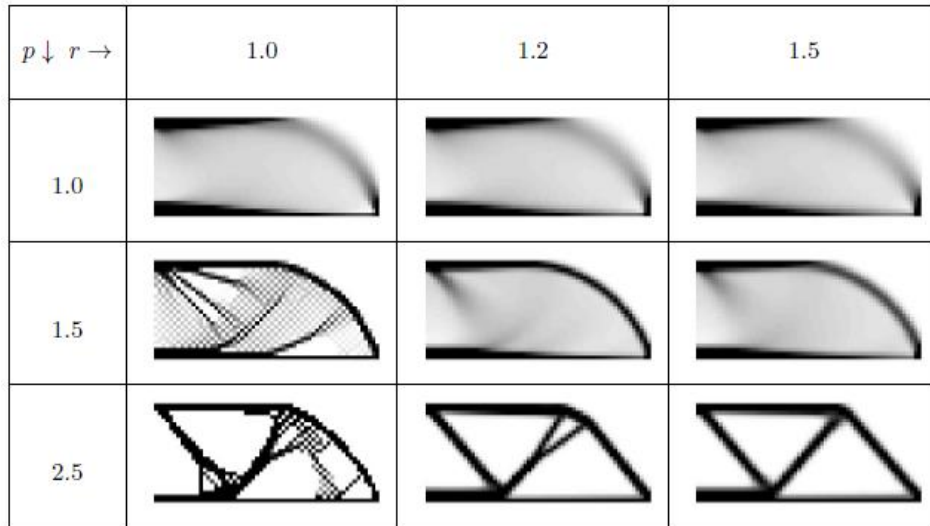


Figure IV.VI Effect of penalty factor and sensitivity filter in a 2D optimization problem.

The parameter on Optistruct that takes into consideration the penalty factor is called DISCRETE. It corresponds to:

$$DISCRETE = p - 1 \quad (IV.VIII)$$

The table IV.I shows the recommended values depending on the type of problem; that is, if the component to be optimized is a solid or a shell and if the MINDIM (Member Size Control) constraint is present, which is a manufacturing constraint. MINDIM takes into consideration the sensitivity filter r , and it represents the minimum size of 2D members in all directions (applied to avoid the checkerboard phenomenon). It is recommended that MINDIM be at least 3 times, and no greater than 12 times, the average element size. By default, DISCRETE is 1 for dominant shell structures and 2 for dominant solid structures with active MINDIM and no other manufacturing constraint. For non-solid dominant models, when minimum member size control is used, the penalty starts at 2 and is increased to 3 for the second and third iterative phases. This is done in order to achieve a more discrete solution. For other manufacturing constraints such as draw direction, extrusion, pattern repetition, and pattern grouping, the penalty starts at 2 and increases to 3 and 4 for the second and third iterative phases, respectively.

MODEL	DISCRETE	PENALTY
Shell dominant structure	1.0	2.0
Shell dominant structure + Member Size Control only	1.0	1 st phase: 2.0 2 nd phase: 3.0 3 rd phase: 3.0
Shell dominant structure + other manufacturing constraints	1.0	1 st phase: 2.0 2 nd phase: 3.0 3 rd phase: 4.0
Solid dominant structure	1.0	2.0
Solid dominant structure + Member Size Control only	2.0	1 st phase: 3.0 2 nd phase: 4.0 3 rd phase: 4.0
Solid dominant structure + other manufacturing constraints	1.0	1 st phase: 2.0 2 nd phase: 3.0 3 rd phase: 4.0

Table IV.I Default DISCRETE and Penalty values for Topology Optimization

A contribution of considerable importance, as well as these two defined parameters, which affects the optimized component is also the quality of the mesh, which, in many problems, the thicker more the optimized beams of the piece are well-defined.

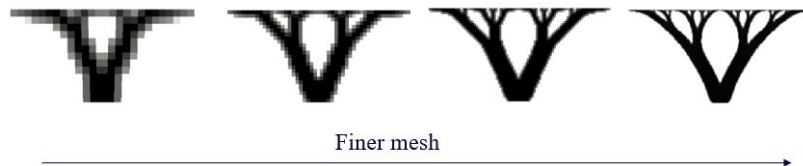


Figure IV.VII Effect of the mesh on the optimized structure

IV.II.II. RAMP Method

An alternative to the SIMP method is the RAMP (Rational Approximations of Material Properties) method. Presented in [21], the method was formulated to overcome the problem of design-dependent loads, such as those of pressure. When the element density is updated, the initial surface properties of the design vary, and the loads are no longer unique.

Thus, it is possible to use a mixed displacement pressure formulation, defining the vacuum phase as an incompressible fluid that is able to transfer pressure loads without further parameterizing the surface [22].

IV.II.III. Homogenization Method

The main idea of this method is to introduce the density variable of the material as if it were a microstructure, or a composite with an infinite number of extremely small voids [23]. This means having a porous composite with a density that varies between 0% and 100%. Some types of microstructure are present in the figure IV.VII. Microstructures alone provide a certain value of penalization on intermediate densities, but this, most of the time, is not sufficient, so it is necessary to insert additional penalization. In addition to having the voids as a variable, for these microstructures also the rotation, and therefore the orientation of the layers, represents a variable, since

the properties are not isotropic. The iterative optimization process proceeds like the SIMP, with the design variables (hole sizes and rotation) assumed as constants on each element. A disadvantage of this method is certainly the greater presence of design variables per element. More information is provided in [23,24,25].

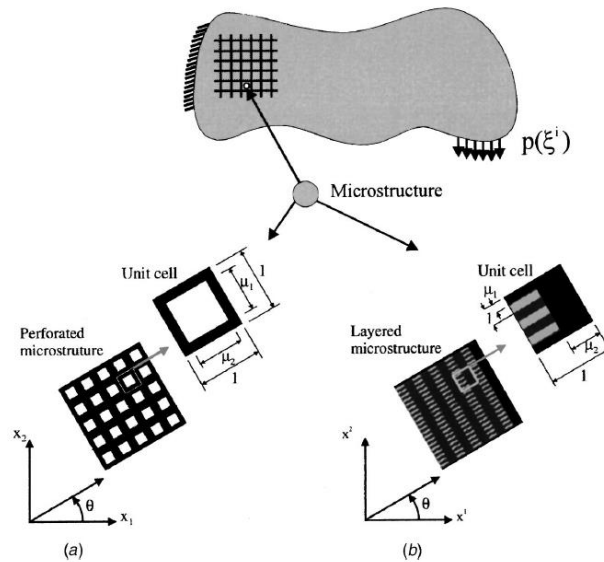


Figure IV.VIII Examples of microstructures with rotation: a) Rectangular holes and b) layered

IV.III. Shape Optimization

Shape optimization is used to improve the shape of a pre-existing component, where the external boundaries of the structure are modified to solve the optimization problem; in particular, using a FEM, the shape is defined by nodal points whose location is modified by the shape optimization, in order to modify it. The design variables, therefore, are represented by a set of geometric parameters, such as the connection radius, the cross-section etc... as they characterize the external boundary of the component. As mentioned, in the finite elements, the shape of the structure is defined by the nodal coordinates, and therefore by the vector of the nodal coordinates themselves \mathbf{x} . When the shape of the structure changes, this must also be translated into a mesh change.

The two main approaches that allow the mesh to be adapted to the change of the component boundaries are (both associate the changes with a combination of vectors):

- The *basis of the vector approach*: the structural shape is defined as a linear combination of basis vector that define nodal locations

$$\mathbf{x} = \sum_i \mathbf{d}_i \mathbf{b}_i \quad (\text{IV.IX})$$

Where \mathbf{b}_i and \mathbf{d}_i are the basis vector and design variable respectively.

- The *perturbation vector approach*: the structural change is defined as a linear combination of perturbation vectors that define changes of nodal locations starting to the original FEM.

$$\mathbf{x} = \mathbf{x}_0 + \sum_i \mathbf{d}_i \mathbf{p}_i \quad (\text{IV.X})$$

Where \mathbf{x}_0 is the vector of nodal coordinates of the initial design and \mathbf{p}_i is the perturbation vector.

As it can be seen the next figure, the section of the beam decreases as you move away from the joint following the optimization of the shape, with a consequent decrease in volume but without changing the mechanical properties.

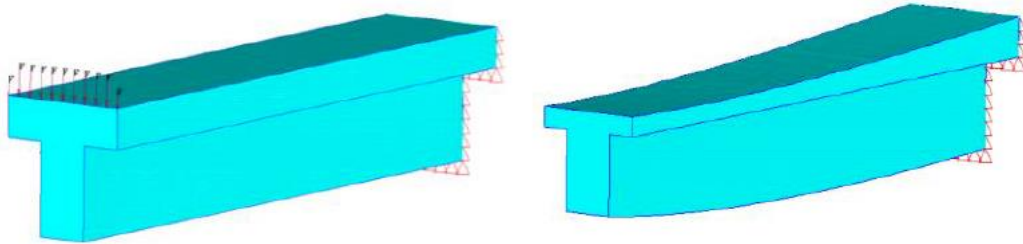


Figure IV.IX Shape optimization of a cantilever T-beam before (on the left) and then (on the right)

IV.IV. Topography Optimization

Topography optimization is an advanced form of shape optimization, in which the variable design is no longer the density that oscillates between 0 and 1 as in topology, but it is a shape variable, more specifically, the offset of each element from its mid plane. The design region is divided into a substantial number of shape variables that allow the creation of any reinforcement pattern, that are beads or swages. This optimization is recommended for thin structures or shells, where mass addition or removal is not required.

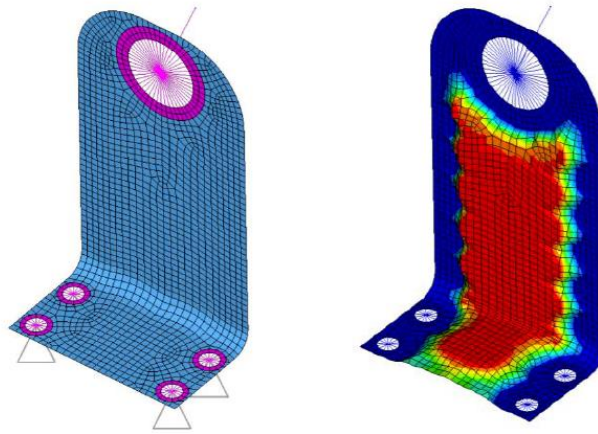


Figure IV.X Topography optimization of a L-Bracket.

The shape variables are the minimum bead width and draw angle. Each shape variable topography has a central circular region with a diameter equal to the minimum bead width; the grids within this region are perturbed and generate a reinforcement bead of depth equal or less to the chosen minimum bead width.

The optimal value of the minimum bead width is between 1.5 and 2.5 times the width of the average mesh element.

In Optistruct there are three methods to automatically generate the shape variables for the topography optimization. The first two differ in the normal which indicates the direction on which to build the bead (element normal and draw vector); the third one requires the input data of each shape design variable by the user.

The draw angle, instead, defines the angle of the sides of the beads and it is recommended between 60 and 75 degrees.

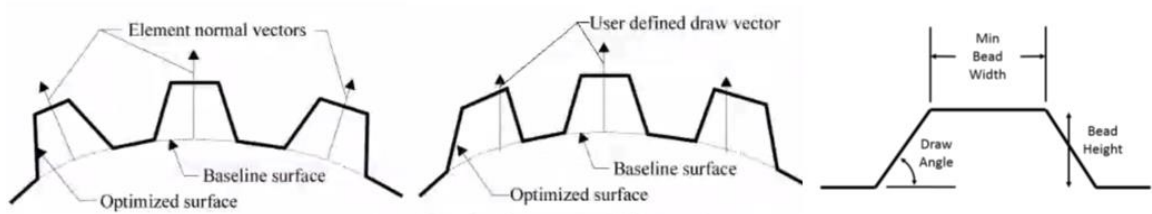


Figure IV.XI On the left beads created using the element normal method; on the centre beads created using the user defined draw vector method; on the right the shape variables of a bead.

IV.V. Free-Shape Optimization

Free-shape optimization is always a shape optimization, with the difference that the nodes of the structure boundaries are free to change their position, according to the optimization constraints and the objective, without defining the perturbation vector.

The design regions therefore also this time are defined through the edge nodes of the mesh. For shell structures, grids move in the normal direction of the edge of the surface while remaining in the same plane, while for solid structures, they move in the normal direction of the surface. During the free-shape optimization, iteration after iteration, the normals change direction following the change of shape, so the nodes will move in the direction of the updated normal. This type of optimization is optimal, for example, in cases where you want to change the shape of the edges of a component where stress is high.

On Optistruct five basic parameters are available to control free-shape optimization, or rather the movement of mesh nodes:

- *Direction constraints* (DTYPE): they provide a constraint on the direction of the grid points defined into design region of the free-shape optimization. They are three: GROW, the inside direction is constrained; SHRINK, the outside direction is constrained; BOTH, grid points are free to move.

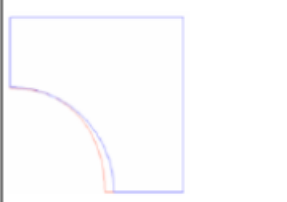
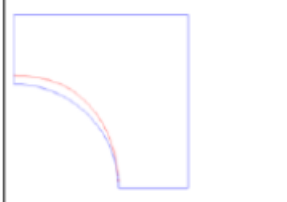
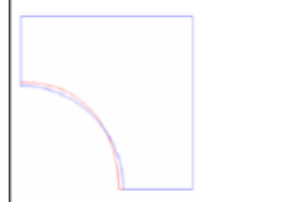


		
GROW	SHRINK	BOTH
	Undeformed	
	Deformed	

Figure IV.XII Direction type on Optistruct available for grid points.

- *Move factor (MVFACTOR)*: it is the maximum allowable movement in one iteration of the grid points, and its value is $MVFACTOR \cdot mesh_average_size$. The smaller is this value, the slower will be the free-shape optimization, but with more stability.
- *Number of layers for Mesh Smoothing (NSMOOTH)*: it is the number of internal grid points, adjacent to those defined into design space, that can be moved to avoid mesh distortion.
- *Maximum shrinkage and growth (MXSHRK and MXGROW)*: they limit the total amount of deformation of the free-shape design region.
- *Additional treatment to grid points in the transition zone (NTRANS)*: a transition zone between design and non-design grid points can be defined to help the smoothing.

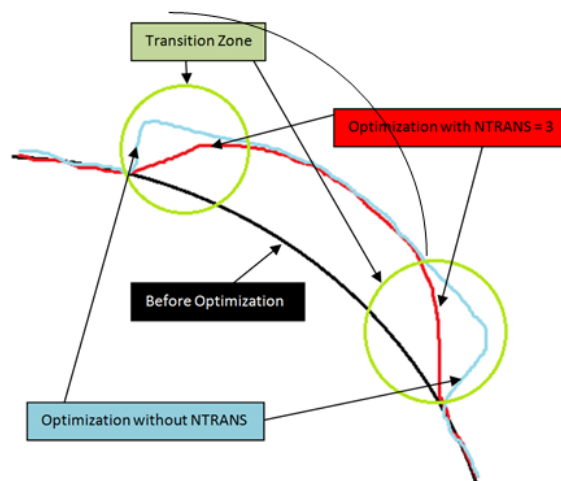


Figure IV.XIII Effect of transition zone definition on free-shape optimization.

IV.VI. Size Optimization

Size optimization is based on changing the properties of structural elements such as shell thickness, spring stiffness, beam cross-sectional properties and mass. Some structural elements have many parameters that depend each other; for example, the beams have the area, the moment of inertia and the torsional constant that depend on the geometry of the cross-section. Thus, in size optimization, the property itself is not a design variable, but the property is defined as a function of design variables. A simple relationship is a linear combination of design variables to express the property:

$$p = C_0 + \sum_i d_i C_i \quad (\text{IV.XI})$$

p is the property to be optimized and C_i are linear factors. For a shell structure, an even simpler relationship places the equality of its thickness with the i -th design variable $T = d_i$.

There are also more complex relationships that link the property with design variables (e.g. with trigonometric functions).

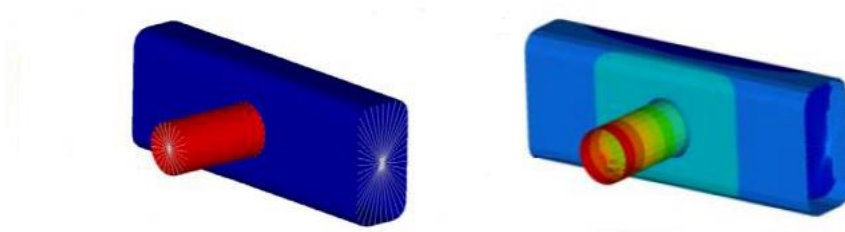


Figure IV.XIV Shell thickness distribution before (on the left) and then (on the right) the size optimization.

IV.VII. Free-Size Optimization

Free-size optimization is a method that allows you to modify the thickness, element by element, of a meshed shell (2D structure). The thickness therefore will not change uniformly, but locally, for each single element, having first defined a thickness interval between T (maximum) and T_0 (minimum). So, the design variable is the thickness of

the element that is free to change in the defined interval, depending on the constraints and the optimization objective.



Figure IV.XV Shell cross-section and minimum/maximum thickness of the shell element.

The continuous variation of the thickness of the structure allows free-size optimization to be more advantageous than topology one. The fact that the latter leads to the generation of optimized components whose elements of the mesh exist or do not exist (0-1 problem) can sometimes be disadvantageous; in free-size elements of intermediate thickness can be obtained, while in topology they must not exist otherwise there would not be a compact structure. The reason why, then, the free-size is less used is strictly linked to the manufacturing of the optimized component. In conventional machining techniques, constructing sheets of variable thickness is not easy and not feasible. In the ambit of AM too, some thicknesses can exceed the technological limit (e.g. laser spot larger than the same thickness). In the next figure a free-size optimization of a wing rib is reported.

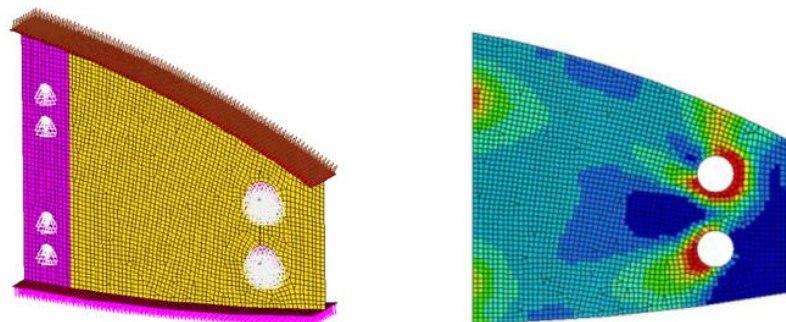


Figure IV.XVI Free-size optimization of a wing rib. Red elements are unchanged thickness, blue elements have thickness equal to 0.

IV.VIII. Lattice Structure Optimization

Lattice structure optimization has been implemented as an extension of topology and it has been developed to assist the innovation of design for additive manufacturing. In fact, as will be seen in the next chapter, there are particular supports that are in lattice form which, thanks to their exceptional strength / weight ratio, are increasingly being studied.

The lattice structure optimization is divided into two phases:

- Phase I: topology optimization is performed with the penalty p not too high, so, to have elements of intermediate density, comparable to areas of porosity.
- Phase II: these areas of porosity (elements with intermediate density) are transformed into lattice structures in compliance with the constraint conditions. Design constraints can be defined in both phases.

The optimized component will therefore be characterized by solid areas and areas consisting of reticular structures. In Optistruct two versions of lattice structures are available, which are tetrahedron and pyramid / diamond cells and which are repeated periodically depending on the 3D mesh of the initial design. The following applies to these types of cells:

$$E = \rho^{1.8} E_0 \quad (\text{IV.XII})$$

therefore, it can be noticed that the penalty factor is equal to 1.8 and E_0 is the Young's modulus of the dense material. If, on the other hand, a high presence of lattice structures is desired, the penalty factor can also be set to 1.25 or even to 1.

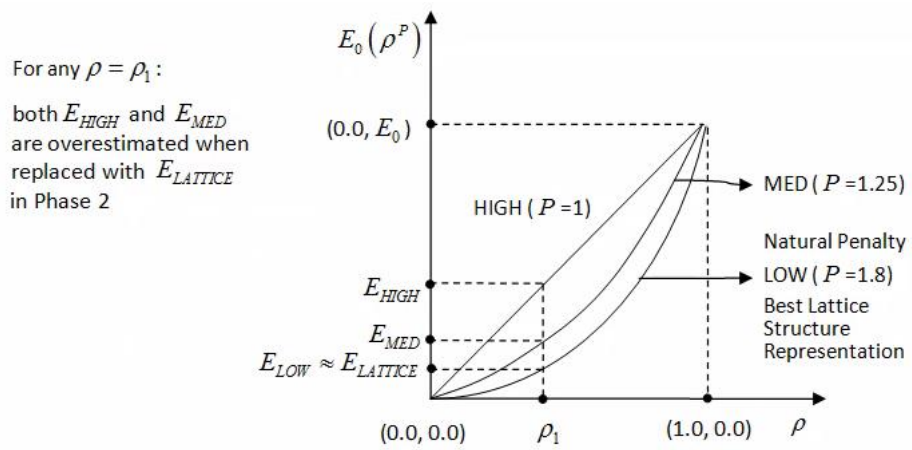


Figure IV.XVII Difference between low, medium and high presence of porosity and their influence on stiffness performance (see equation IV.V).

The lattice structures are RODs and their cross-section can be constant as can also be variable along their axis, thus obtaining tapered beams. The diameter of the section of the ROD element is in any case proportional to the density of the replaced element.

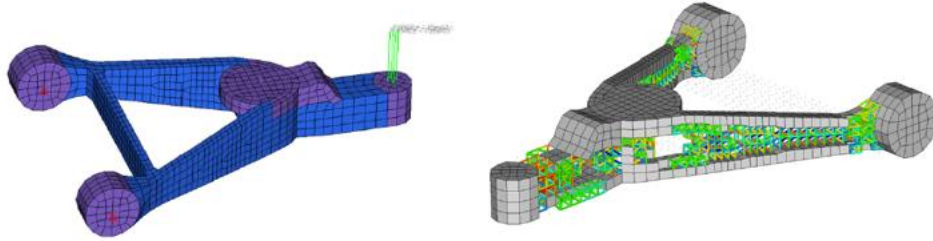


Figure IV.XVIII Lattice structural optimization of a Control Arm with tetrahedral elements.

V. Support structures

Being this thesis projected on the optimization of the supports, it is important to make an overview on their functionalities, characteristics, impact on process chain and an analysis on which are the most used types in the AM techniques, particularly PBF, which allow the success of the process of production. The possibility of generating increasingly complex forms using AM has been analyzed. This means that elements such as supports are necessary for the purpose of production success, even if their presence has become inevitable since the birth of rapid prototyping. In addition to benefits, they also involve an increase in production time, an increase in material used, an increase in energy consumption and a component post-processing: all this is therefore reflected in an increase in cost and manual intervention by part of the operators. Consequently, if their presence is inevitable, trying to reduce them as much as possible is necessary.

As can be seen from Fig. V.I, in the last 28 years research has led to an ever-increasing number of publications: on the other hand, in parallel to this, even the publications on support strategies increase. This is because with the emergence of new AM technologies, the strategies change [27].

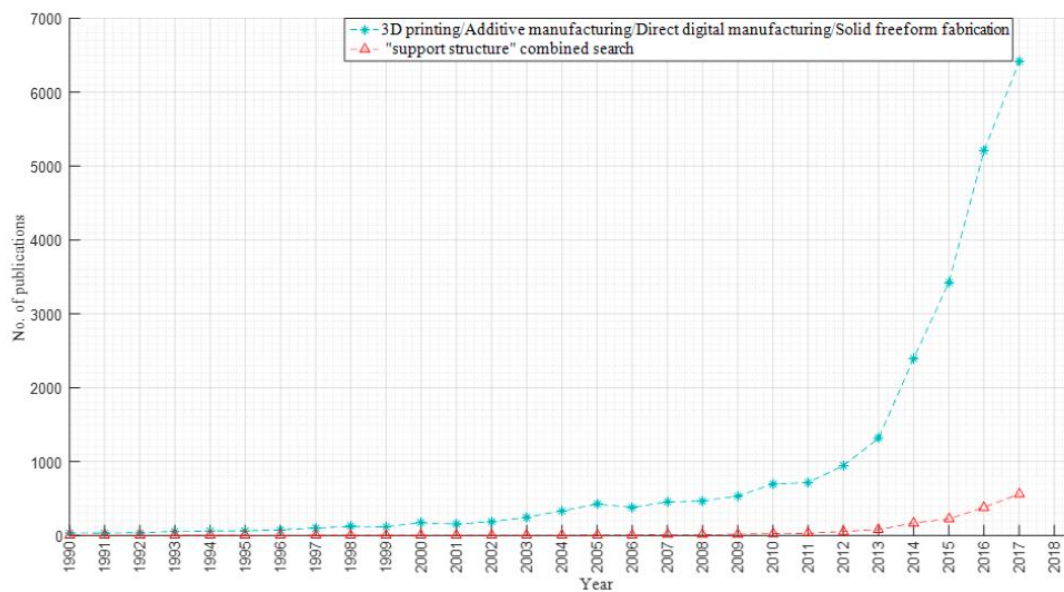


Figure V.I Number of published papers for AM and Support Structures.

V.I. AM technologies & Support Structures

Each technology requires the presence of supports for different reasons. Overall, the main purposes of these structures are three:

- *Heat diffuser and rigidity enhancer*: especially for metal processes PBF, there are high thermal stresses on the part that cause distortions and residual stress. The supports must balance these negative behaviors during and after printing.
- *For printability*: some AM technologies can deposit material (if DED) or melt powder (if PBF) only if on surfaces already generated or pre-existing; therefore, the supports are necessary so that the first layer of a surface of the part that is being generated, if at a different height than the others, can be found below material.
- *For balance*: components of geometry, can have self-sustained surfaces but also particular shapes that are not able to be perfectly balanced, or that cannot be supported by other parts of the component itself; in this case a support structure can act as a fixture.

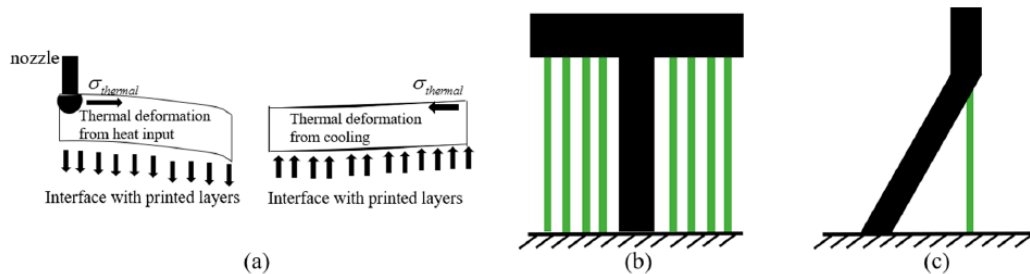


Figure V.II a) stress gradient during melting and stress residual after cooling; b) support structures (green) for printability; c) support structures for balance.

At the same time, as already anticipated in the introduction of this chapter, as the supports solve certain problems, they bring with them new challenges. So, there are many disadvantages:

- *Setup STL*: during the setup of the STL file, choosing the orientation of the part is fundamental to reduce the quantity of material destined to the support; this then requires a lot of attention, time and experience of the operator.
- *Increase of manual work and surface finish of the component*: supports can also be removed manually. This requires additional time for process chain. Moreover, even if removed, they leave what is called “witness” on the surface of the part, which must therefore be subjected to polishing to have the roughness in the required engineering tolerances. All this above all in processes with metallic materials
- *Non-reusable material*: obviously the supports are of material no longer reusable, as they have already been subjected to the AM process. Therefore, all the material that is used for the generation of the support structures must be taken into consideration of the cost cycle, because it is to be discarded.
- *Time-Energy*: Being the supports an additional material to be printed, this is reflected in a substantial increase in production time and consequently in an increase in energy that is proportional to the volume of material to be used.
- *Design of the part*: Extra time is required to make a design of the part that is able to accommodate the support structures as well as the design of the support structures themselves.

The following table takes into consideration the AM techniques for more used metal materials and if they require the presence of supports and above all for what purposes.

AM technology	Type	Need of Support Structures	Functions of Supports		
			Heat diffuser	For printability	For balance
PBF-Powder bed fusion	SLM	Yes	✓	✓	✓
	SLS	Not always	✓	×	×
	EBM	Yes	✓	✓	✓
DED-Directed energy deposition	DMD/LENS	Yes	✓	✓	✓
	LPD	Yes	✓	✓	✓
	SLC	No	×	×	×

Table V.I Some of AM technologies and need of support structures.

V.II. Support Structure Methods in AM

It was therefore understood that the support objective is hold parts during its printing to make ensure that the part remains in the planned position. In this paragraph all main methods to minimize the generation of the supports and maximize their efficiency are analyzed. From Fig. V.III, it can be noted that two paths can be followed; one leaving the shape of the part unchanged and a second one exploiting the optimization methods to modify the part itself as required. The second path is substantially as seen in the design for additive, where topological optimization is used to preserve the same properties (or improve them) with less material and distributed differently to the component; with this perspective, numerous factors can be taken into consideration, including the generation of self-supported surfaces for a certain orientation that the original component did not have in order to reduce the use of supports.

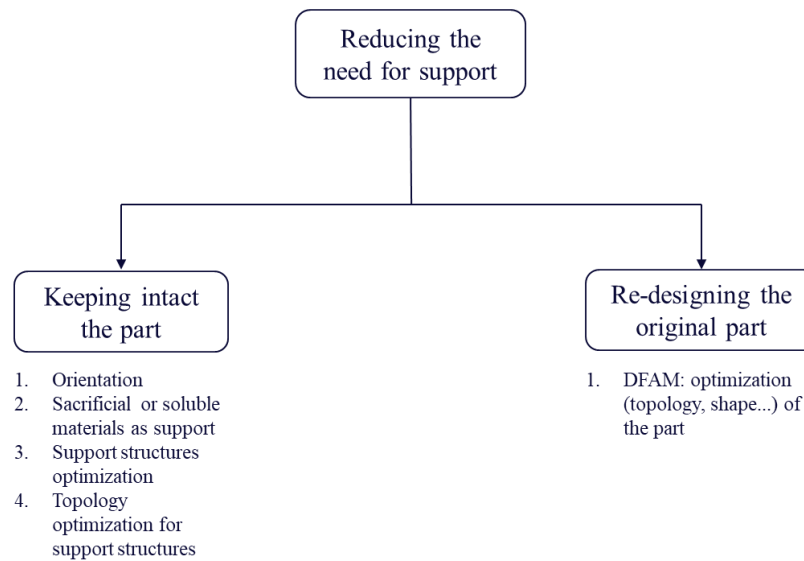


Figure V.III Methods to reduce the presence of supports.

Before describing the factors that minimize the number of them or the methodologies to generate advanced supports, we analyze the structure of a *classic one* and the *principles of their design*.

A *classic support* is constituted as in Fig V.IV. It is composed of two parts: teeth, which are the connection between the part and the support and serve to minimize the

contact area (and therefore the witness) and to facilitate removal and the main body. Having distant teeth facilitates removal but involves a worse surface finish and distortion of the part, and vice versa if they are closer. Many factors must be taken into consideration when designing the support structures as well as the distance between the teeth, such as the tooth top length, tooth base length, tooth height and offset (penetration in the part).

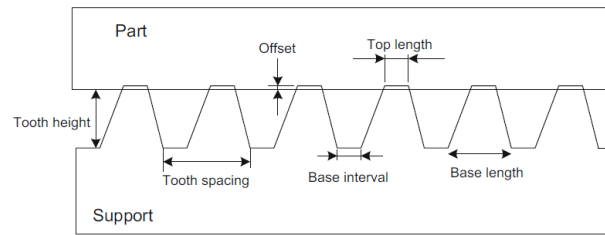


Figure V.IV Teeth of a support structure and its characteristics.

The main block of the support is usually also unpacked into many small supports in the shape of parallelepipeds to facilitate removal and it should be strong enough to withstand both the vertical weight and other horizontal disturbances. For the support geometries shown in Fig. V.V, there exist some general guidance. For example, block support is usually used for bulk geometries, while point and line supports are used for small features. Contour support can be considered when the contours of the parts need to be better sustained [28].

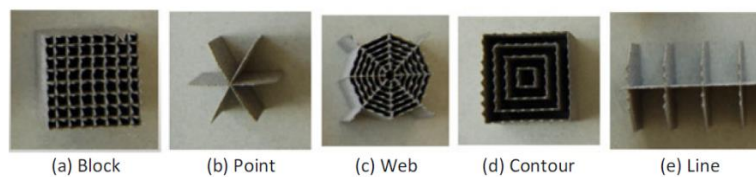


Figure V.V Examples of different types of support structures.

Generally, during the DFAM, we base on the following main rules for the design of the supports:

- avoid large diameter holes parallel to the printing direction;
- avoid surfaces with too high overhang angles;
- avoid surfaces in positions where the support will be difficult to remove.

The consequence of these rules is that the freedom so offered by many AM technologies begins to be more limited.

At the same time, the design of the supports is based on certain principles, and it is itself subject to restrictions, such as overhang angle (it would make no sense to support what must act as a support). Therefore, the *principles of support design* must be the following:

- The support should be able to prevent parts from collapsing and warping, especially the contour area of the part. For design, especially in the process of processing metallic materials, deformations and thermal stresses must be taken into consideration through thermal analysis;
- The contact area should be as small as possible to reduce the “witness” left on the part surface after removing the support;
- The connection between the support and the part should be of minimum force, to guarantee easy removal;
- Material consumption and build time must be considered as a significant factor, as well as the compromise between them and the final print quality.

There are a lot of software for the generation of supports including CURA, Slic3r for FDM and Magic for metallic PBFs. Another way is the manual CAD design.

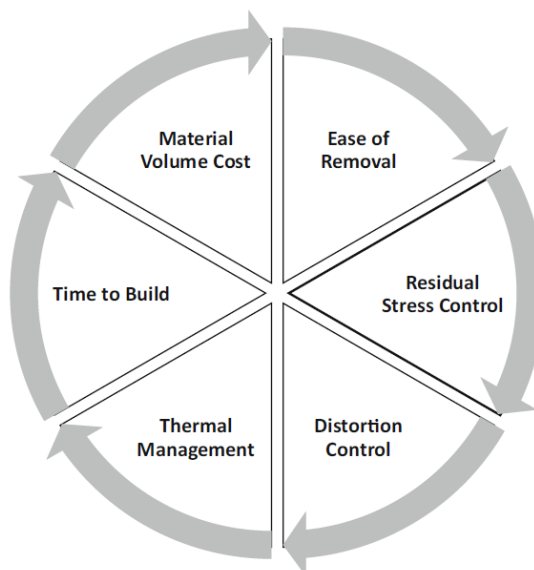


Figure V.VI Consideration for Support structure design.

V.II.I. Orientation and overhanging surfaces

The build orientation refers to the direction orthogonal to the layers that will form the component. AM part orientations play an important role in AM processes as they have a profound influence on the properties of the final part and the nature and amount of support structure needed [29]. In fact, it influences the surface roughness, the contact surfaces with the supports, the construction time and the cost. In AM process, it is considered an overhanging structure a part of a component that is not supported during building, by solidified material or a substrate on the bottom side. Consequently, the melt pool created by the heat input from the laser is supported by powder material [30]. It is necessary to avoid as much as possible surfaces that are in overhanging during printing (problems can be the staircase effect, dross formation and warp, Fig V.VI). One solution is to orient them to be in a certain inclination. In fact, depending on the material used, a surface can be self-supported, in general, if it is inclined at $30^\circ/45^\circ$ or more to the direction of the layer horizontal axis (Fig V.VII); this reasoning, however, turns out to be increasingly difficult if a component with a very complex shape is to be created, in which there will inevitably be surfaces to be supported.

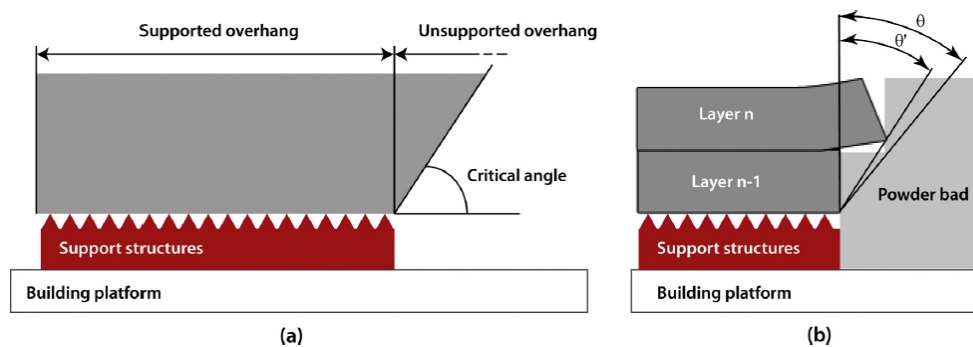


Figure V.VII(a) Supported and unsupported overhang features at a critical angle θ and (b) warping principle in the second one: the effective inclined angle θ' between the overhanging part of the layer and the previous layer is smaller than the designed inclined critical angle θ .

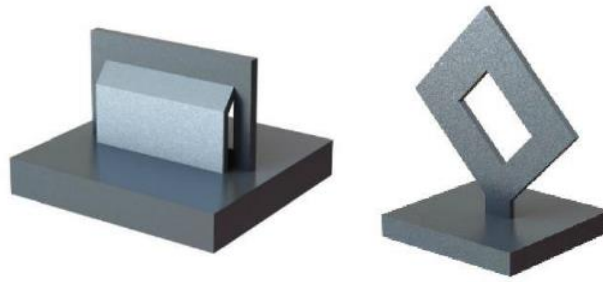


Figure V.VIII A simple part built with supports on the left. The same part without any support on the right (little support only for EDM) built at 45°.

Generally, the orientation is defined when the file is converted to STL, where the software recommends the one with the least area to support. Experiments regarding the concavity and convexity of the unsupported surface can be well analyzed in [30]. In general, to be conservative, it is convenient to support the convex or concave surface when the tangent to it is inclined $30^\circ/45^\circ$ with respect to the horizontal (layer direction). Holes with diameters less than 6mm, regardless of orientation, do not require supports; while if they have a slightly larger diameter they may present unacceptable surface roughness.

The cycle for choosing the appropriate orientation is shown in the figure V.IX.

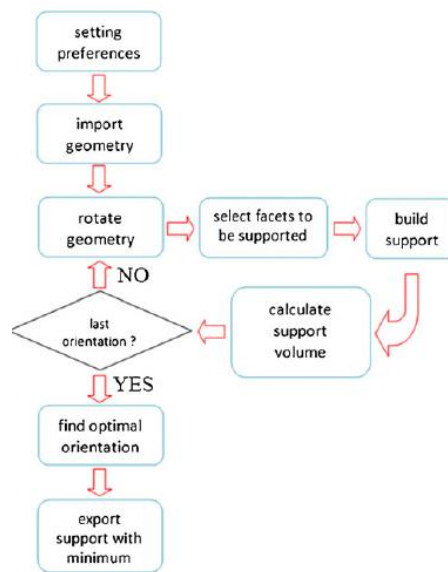


Figure V.IX Schematic of first step optimization for optimal orientation to reduce support volume

V.II.II. Sacrificial or soluble materials as support

One method to reduce the consumption of primary material destined for the production of the part is to use a secondary material that is soluble or expendable in some way to make the supports. Sacrificial material means a material that can carry out the work on the support and that allows greater ease of removal. This technique has been widely used in FDM (Fused Deposition Modeling) techniques, and on rare occasions tested in DED metal [31] but is very difficult to apply in PBF techniques since a large phase of machine setting and post processing are required. In the FDM the supports are generated very often with soluble material, particularly polymers which are solubilized with water, alcohol (e.g. isopropyl) and hydrocarbons (e.g. limonene).

V.II.III. Support structures optimization

The various types of optimized supports described below have been tested, or are currently applied, for AM technologies with metallic powder, particularly PBF. The need to reduce the volume fraction of the supports, and therefore the build times and costs, but which always have good thermo-mechanical properties, has led to the use of more optimized structures, including cellular support structures, also called lattice. Mainly two cellular structures have been studied, called (Schwartz) Diamond and (Schoen) Gyroid, and it has been shown that the construction time has been reduced satisfying the structural demands [32].

They are defined around a single volume cell, and by exploiting their periodicity, this cell is repeated n-times until the entire volume subtended by the overhang surface is filled. Thanks to their periodicity, interconnection between repeated cells is guaranteed. Considering a single cell, their surfaces are defined by these equations:

$$\text{(Gyroid)} \quad \cos(x) \sin(y) + \cos(y) \sin(z) + \cos(z) \sin(x) = 0 \quad (\text{V.I})$$

$$\begin{aligned} \text{(Diamond)} \quad & \sin(x) \sin(y) \sin(z) + \sin(x) \cos(y) \cos(z) \\ & + \cos(x) \sin(y) \cos(z) \\ & + \cos(x) \cos(y) \sin(z) = 0 \end{aligned} \quad (\text{V.II})$$

However, an excessively low volume fraction can be too fragile to be produced consistently with an SLM process with the desired resolution.

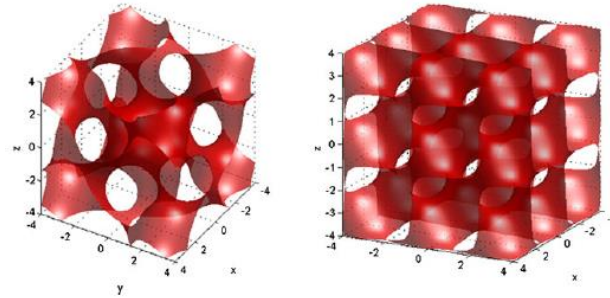


Figure V.X From the left, Gyroid and Diamond lattice structures in a 4x4 cell.

Another particular lattice structure is the Unit Cells Voxels used for support generation. With the same logic of separation of the volume in n-cells described above, an octahedral truncated (14 faces) or rhombic dodecahedral structure (12 faces) is repeated. The advantage compared to the previous lattices is that it is not necessary to fill the entire volume discretized in cells, as their faces inclined at 45° (in respect of which the support itself does not become an overhang surface) give greater flexibility of construction in any direction. The aim is to intensify the presence of the Unit Cells Voxels near the part to be supported, and instead reduce it by going to the build plate [33].

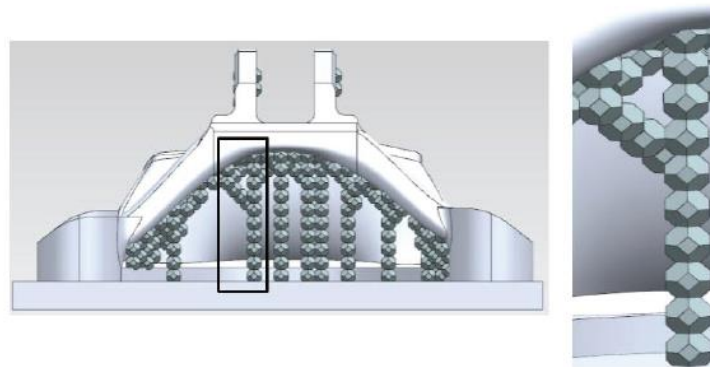


Figure V.XI Example how Unit Cells Voxels generate a support structure.

According to [34], “IY”, “Y” or Pin-shaped structures support overhang surfaces with good results; in fact, it has been verified that with only 2.2% of contact between supports and part an acceptable surface roughness can be obtained, uniformly spacing the IY supports. Another result is that unequal-spaced supports lead to having a different and unsatisfactory heat dissipation model such as to induce deformation in the part.

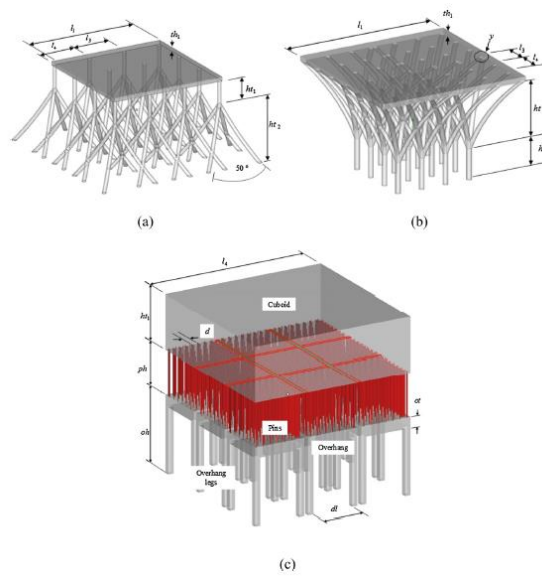


Figure V.XII a) “IY” support structure for a thin plate; b) “Y” support structure; c) Array of Pins support structures.

V.II.IV. Topology optimization for support structures

The topology optimization was used for the most part to optimize the structure of the component to be printed, which, as we have seen, is a mathematical method that allows to optimize the layout of the material in a given design space. The purpose of this thesis is to deepen the integration of the TO in the design of the supports. In this regard, in the following chapter, an innovative model is presented to carry out this integration that exploits the advantages of the TO. Research on the integration of TO for the support structure is still necessary as TO can significantly reduce the necessary support and optimize support structures based on material properties.

An example of a general workflow of topology optimization for support structures is shown in the Fig. V.XIII.

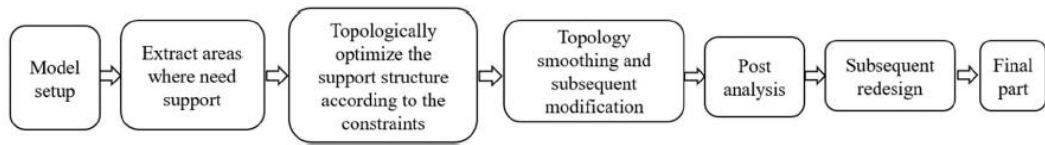


Figure V.XIII A general workflow to execute a TO for support structures.

VI. Generation of support optimization method

As it has been pointed out so far, support structures generation is a crucial point in the AM process chain. Sometimes, the automatic generation of the support by the new software on the market is not satisfactory and the designer's experience is not enough to design them in order to compensate for the problems that the part may present during and after the printing phase. The proposed challenge was to generate a semi-automatic method, which assigned specific data as input, the output must be an optimized support that can be directly applied to the component, or at most with small manual corrections. Therefore, the aim is to reduce the time, since we want to bypass the manual modeling of supports for complex structures, the powder material used, which, as mentioned in the previous chapter, will be discarded, and the thermal deformations that the part may present.

Before the description in detail of the generated system, it is useful to start with clarifications and from the logical scheme that helps to understand the process iteration step by step.

With minor modifications, the scheme, that will be presented, is adaptable to many of the additive manufacturing metal powder technologies that involve the use of supports (see table V.I; a similar work can be well studied in [35] for FDM technology). In this case the reference technology is the Selective Laser Melting.

To verify the validity of the scheme, it was first applied to an invented part not of industrial application, which can be viewed in Appendix.

The product to be printed is a low-pressure turbine blade. The difficulty in generating the supports for this component and the need to reduce the time and costs to produce this piece have led to the modeling of this new process of creating support structures, which, thanks to its flexibility, can be adapted to any component, and therefore can help designers in future new design challenges.

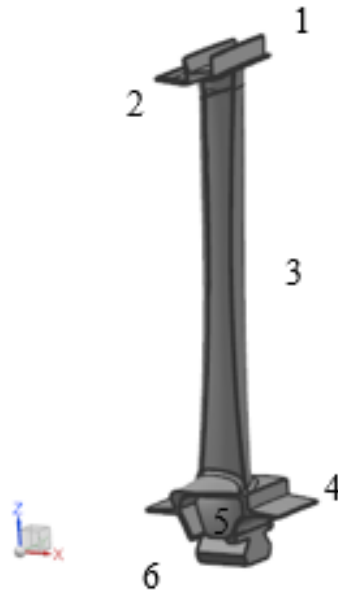


Figure VI.I Low-pressure turbine blade to be printed; 1) Fins 2) Shroud 3) Foil or blade body 4) Angel Wings 5) Shank 6) Fir tree or Dovetail

The intuitive scheme is shown in the figure VI.II. Step by step the iterative process applied to the examined component will be analyzed. Keep in mind that no passage is independent, but that each is linked to the adjacent ones.

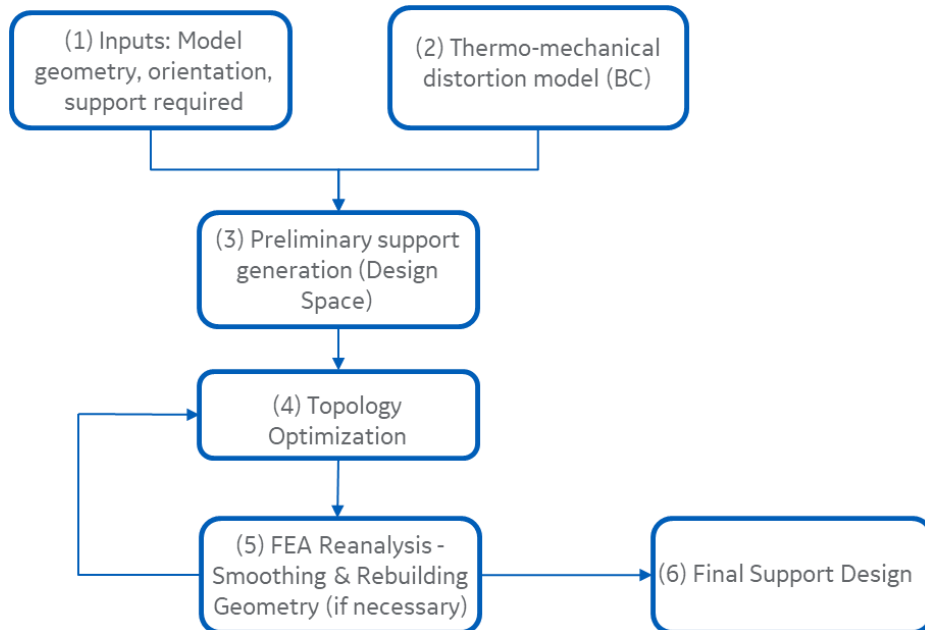


Figure VI.II Logical scheme to execute topology optimization for supports.

VI.I. Model geometry & Orientation

As shown in the figure VI.I, a turbine blade consists of 6 main elements. The function of fins (1) is to reduce flow leakage thru tip of the blade that is driven from a favorable pressure gradient along the flow path, in the meanwhile they also allow thermal growth of blade by rubbing the honeycombs that are brazed on the outer shroud, without any fatal impact on safety running of blades itself. The “zeta” shroud (2) shape is able to guarantee a correct assembly of all row of blades of with a cold interlocking preload that is kept during all engine running in order to prevent any resonance issue. The inner platform (4), also called “angel wings”, has mainly an aerodynamic function, together with airfoils (3), for performances and to prevent any flow leakage from the flow path to the inner cavities of the disk. The shank (5) is mainly the transition zone between the aerodynamic portion and the constraint feature of the blade (fir tree or dovetail, 6). The dovetail is the mating zone with the LPT disk; typically, most stressed locations are in the shank, dovetail and fillet radii between airfoils and inner/outer platforms.

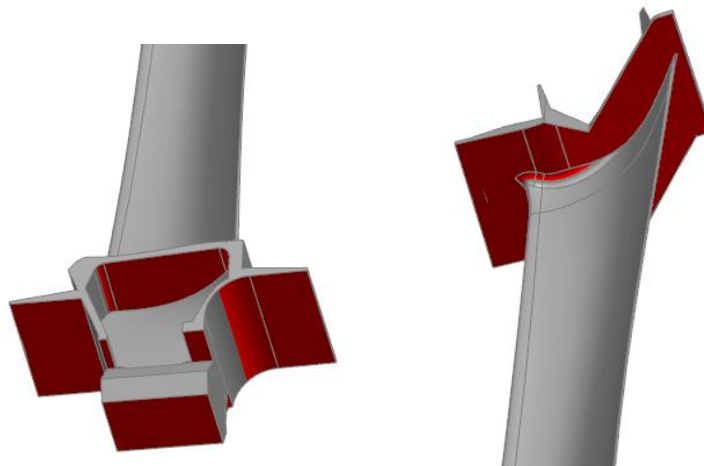


Figure VI.III Individuation of overhang surfaces (color: red). These surfaces will represent the areas of contact between the part and the support.

The choice of orientation is with the stacking axis coincident with the z axis of the machine. In this condition the fins are at an inclination above the considered angle and the foil of the blade, the most important part, does not require any support; consequently, there is no need to rework the airfoil surfaces in order to remove any support witnesses. The configuration, then, requires the support of the lower surfaces

of the shroud flow path side, of the angel wings, of the shank and of the dovetail. Obviously, even the lower surface of the dovetail must be supported because following the EDM cut could remove parent material of the blade; therefore, the first printing layer must be melted for the support (it will be seen in next chapters that the blade is positioned at a minimum distance of 4 mm). These surfaces will represent the areas of contact between the part and the support.

VI.II. Thermo-Mechanical distortion model

The thermo-mechanical distortion model is performed by a software that allows to simulate the printing process. Once the orientation has been chosen, the part must be imported (as STL file) into the Netfabb software without being moved, because, as we shall see, it is essential that the same reference system set in the CAD model is preserved and that it will be the same in the Hypermesh / Optistruct software.

In the software, among the various settings, there is the choice of the AM machine and consequently the size of the plate; during the phase of generation of the preliminary support, as will be seen, it is important that the plate is exactly the same.

It has been seen that the lower surface of the dovetail is a surface to be supported, so it is not possible to carry out the simulation by imposing it in contact with the plate (in the software it is not possible to simulate the printing of the piece "suspended in the air"): to remedy to this problem, an anchor volume was inserted (height of 4 mm, circled feature in Fig.VI.IV), as support, between the surface and the plate with low density and mechanical properties, so that it influences the simulation by little or nothing.

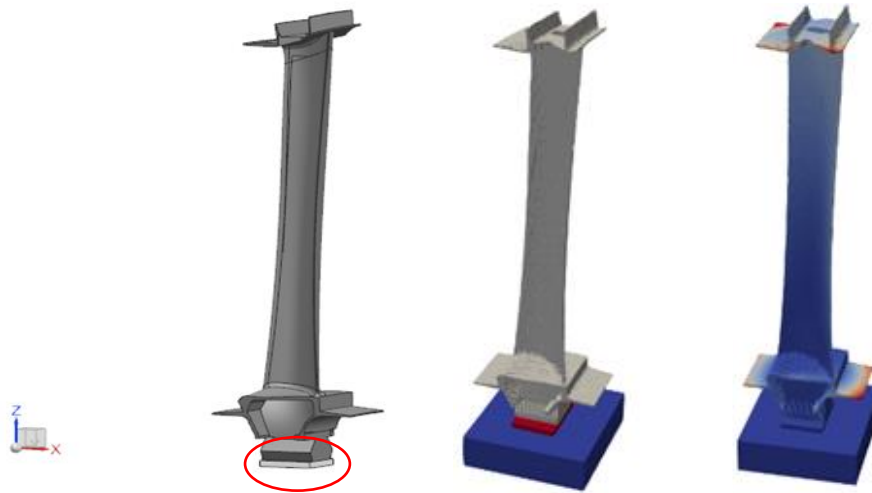


Figure VI.IV Anchor volume with low mechanical property and low density as support into red circle. In the centre the blade with anchorage (red). On the right the simulation and magnitude displacements mapping.

The software, to carry out the analysis, works by discretizing the component into elements. Depending on the desired setting, the elements, which are QUAD, contain "n" layers of melted powder.

As output of this simulation, it is necessary to group in a text file or .xls the coordinates of the mesh nodes and the respective displacements along the three directions deriving from the deformation that the component would present if it were not supported.

VI.III. Preliminary support generation (Design Space)

In this phase it is necessary to define the preliminary support to be applied to the blade. It represents the design space of future topological optimizations, where the algorithm must act in order to generate the load paths distributed with the density method described in chapter IV. The following rules were followed to generate the design space:

- To counterbalance the deformations;
- The intersection of the two DS is avoided;
- Contained in the machine plate.

The design space has been designed in such a way as to counterbalance the displacements of the blade surfaces. To have a general view of the directions towards which the various sections of the component tend to deform, it is useful to represent the displacements on the component itself. The coordinates and displacements exported in the previous step refer to the nodes of the mesh generated by Netfabb; the mesh of the turbine blade, generated on Hypermesh, is characterized by R-TRIA elements. The reason for importing the component from NX to the simulator software without moving it on the plate is intuited in this step; in fact, by doing so, the nodal displacements of the QUAD elements can be linearly interpolated to R-TRIA (Fig VI.V), since the surfaces are exactly arranged in the same points in the working space.

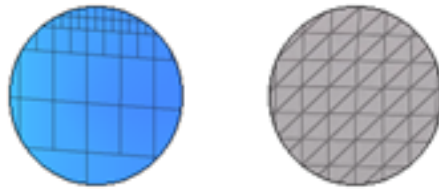


Figure VI.V Detail of a same meshed surface on simulator software (QUAD on the left) and Hypermesh (R-TRIA on the right)

The displacements have been interpolated in the critical points of the blade, or on the areas to be supported (Fig VI.II), and it can be seen in fig. VI.VI and VI.VII.

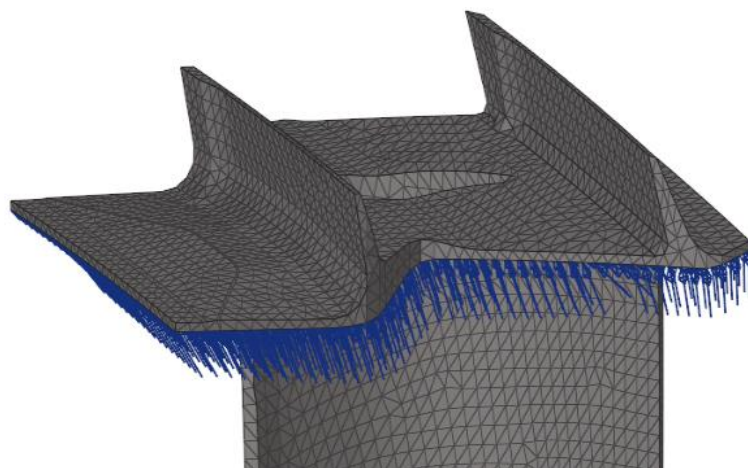


Figure VI.VI Displacements mapping on the shroud surfaces.

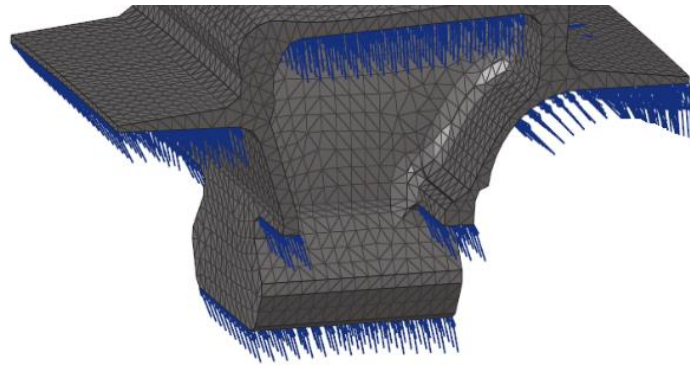


Figure VI.VII Displacements mapping on angel wings, shank and dovetail.

As you can see the design space of the lower part of the blade is wider in one side precisely because we expect that the future load paths that the optimizer generates require more material to support in that direction. Two design spaces were chosen in two levels in order to avoid a single optimized support, making the removal of future supportters less complex. Therefore, these have also been designed in compliance with the dimensions of the AM machine plate (Fig VI.IX).

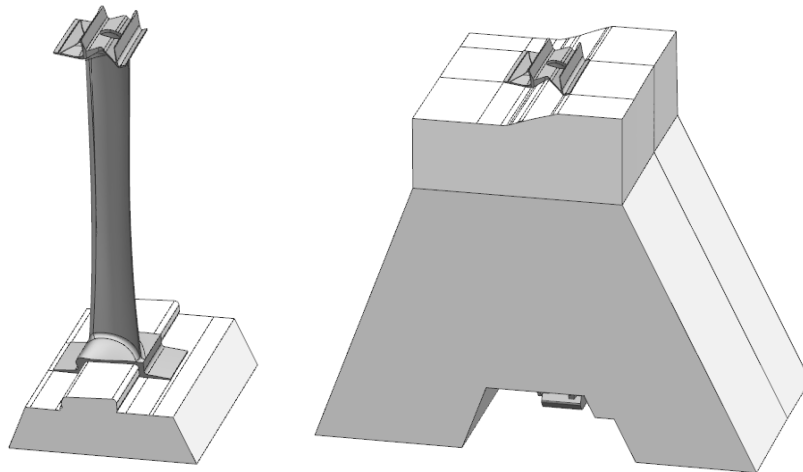


Figure VI.VIII Design Space generation on the top (right) and bottom (left) of the turbine blade.

The choice to generate two design spaces is also closely related to computational computation; in fact, the optimizer has to go and look for the solution in a smaller

volume every time, so having just one design space has led to very long optimizations with numerous iterations. NX Siemens was used as 3D-CAD modeling software.

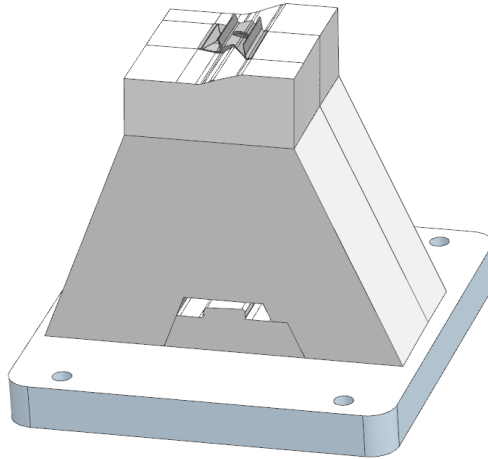


Figure VI.IX Design Spaces on the platform of AM Machine.

VI.IV. Topology Optimization

Before performing topological optimization, it is necessary to set the loads and constraints for the static analysis.

In the contact areas between the support and the blade, as seen in the previous paragraph, the displacements were interpolated on the blade itself in order to have an overall view to generate the preliminary design spaces; this time, being the contact areas at the same height, they are interpolated on the meshed design space. At the same time, to simulate the presence of the plate below the supports, the clamping is placed as a constraint on the entire underlying base.

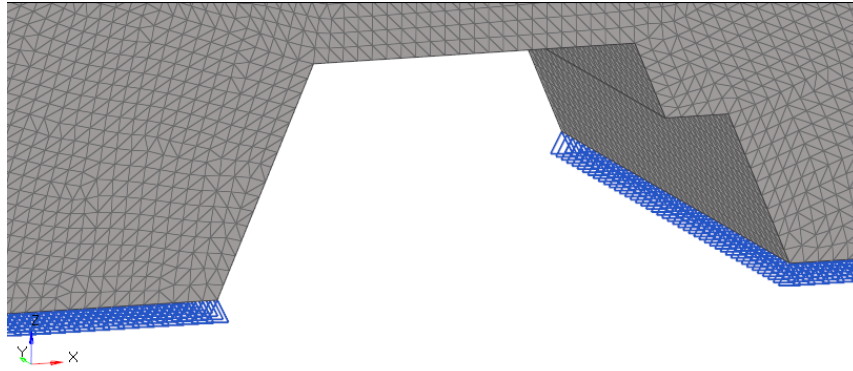


Figure VI.X Detail of constraint under the base of the preliminary support of the shroud.

For the static analysis it would be enough to set these shifts as SPC constraints, however, to optimize you need to have the forces, or rather, you need to derive the forces that generate those certain displacements.

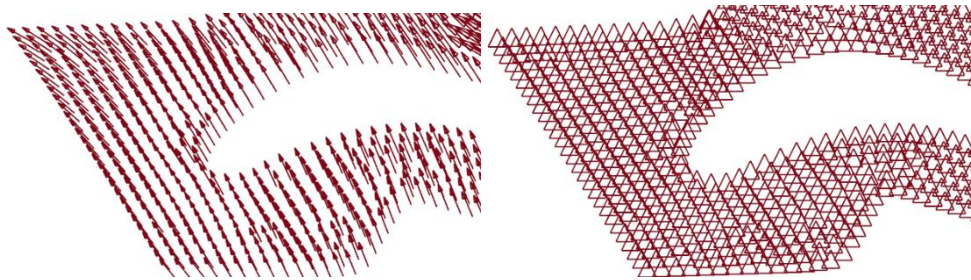


Figure VI.XI Displacements as vector form (left) and as constraint (right) of the preliminary support of the shroud.

To do this, the nodal displacements are imposed as constraints, and through the static analysis we obtain the reactions in those nodes (on Hypermesh they are called SPCF and they are represented on Fig VI.XII). These forces, in essence, represent the forces that the preliminary support undergoes for assigned deformations of the blade.

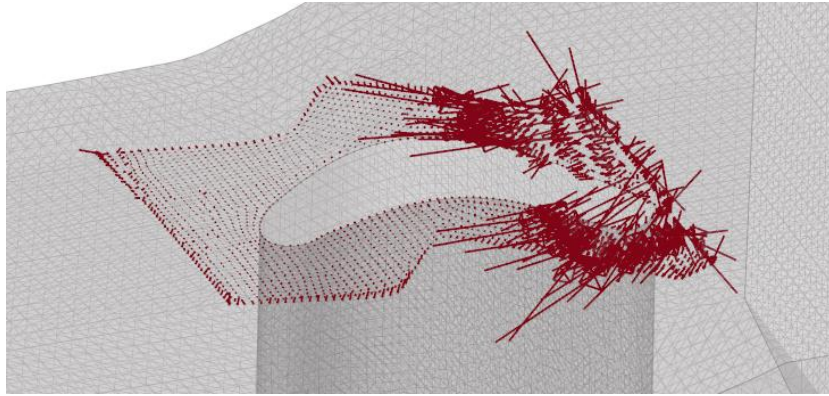


Figure VI.XII Force distribution on the preliminary support for the shroud.

The figures shown so far represent the design space supporting the shroud. Similar considerations were also made for the other design space supporting the angel wings, shank and dovetail, thus obtaining the distribution of the forces as in the figure VI.XIII.

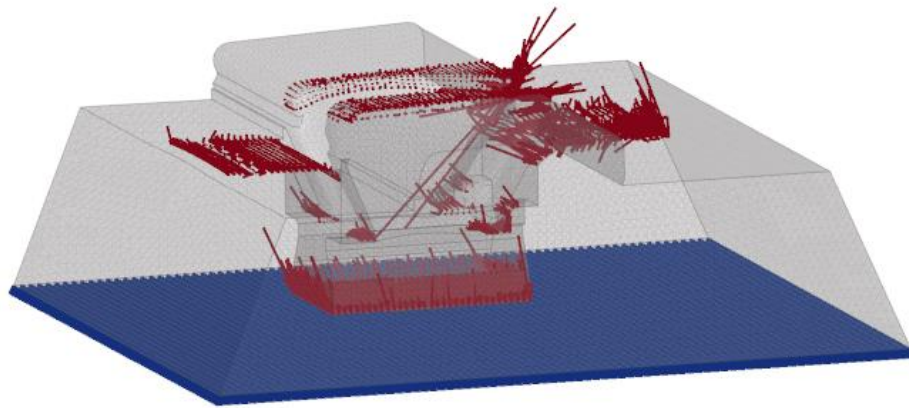


Figure VI.XIII Force distribution on the preliminary support for angel wings, dovetail and shank.

Now everything is ready to carry out the first topological optimization process for the two design spaces. From now on the preliminary support of the shroud will be defined as *Design Space I*, *Design Space II* the other one.

FIRST OPTIMIZATION

Model used	Design Space I
Objective	Minimize Compliance
Optimization Constraint	UB Volume Fraction 0.3 Overhang 45°

The overhang constraint forces the optimizer to generate surfaces for the load paths within a specified angle limit and it has been used because it makes no sense to have surfaces to be supported being themselves supports: in this case the limit was chosen equal to 45 °. With this type of optimization, the software is being asked to generate a configuration with the minimum compliance with the reduction in the requested volume fraction (upper bound, UB, of 0.3 means a 70% of volume reduction). The volume has been set as an optimization constraint since it represents the parameter that influences the time and the cost to produce the support. The choice of MINDIM, instead, as mentioned in the previous chapters is closely related to the mesh; since it is representative of the sensitivity factor, it has been set equal to about three times the value of the size of the average element. DISCRETE see table IV.I.

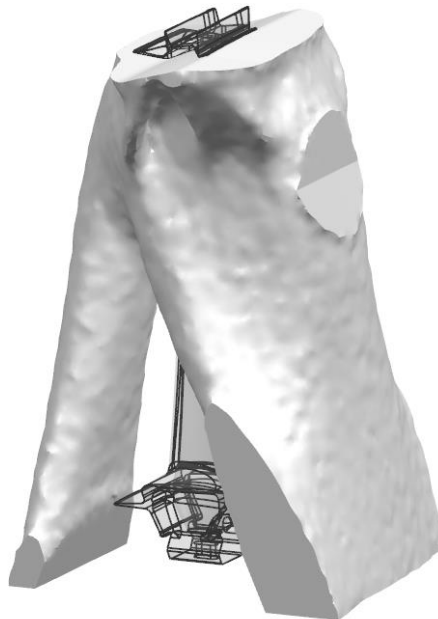


Figure VI.XIV Result of First optimization for Design Space I.

The results and computational cost to obtain the optimized support (represented in Fig. VI.XIV) are:

Volume	-70%
Compliance	+331,4%
Mass	-70%
Threshold	0.5
Iterations	37
Time	3h52

Obviously, the percentage values correspond to an increase or decrease of the variable in consideration with respect to the design space I. The threshold is the filter parameter of the intermediate density of the elements, chosen equal to 0.5, it means that all the elements that have density equal to 0.5 or higher are reported at a density equal to 1 and the remainder equal to 0.

Model used	Design Space II
Objective	Minimize Compliance
Optimization Constraint	UB Volume Fraction 0.3
	Overhang 45°

The same considerations are made as above. The only changed condition is MINDIM due to a different meshing.

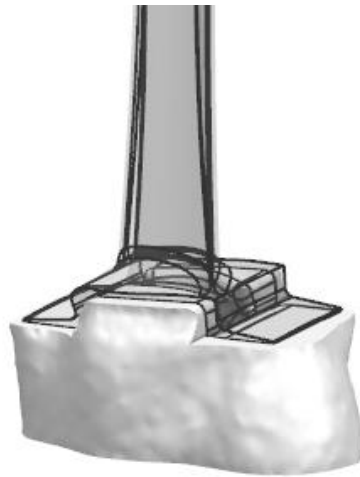


Figure VI.XV Result of First optimization for Design Space II.

Volume	-70%
Compliance	+424,4%
Mass	-70%
Threshold	0.5
Iterations	41
Time	1h25

VI.V. FEA Re-analysis and smoothing

The Optistruct software, at the end of the optimization, provides the *.sh* file necessary to perform the FEA Re-analysis and OSSmooth. The FEA Re-analysis allows to automatically set the same previous problem, however, on the optimized supports (which will be, therefore, the new design spaces), leaving the forces unchanged in the same nodal coordinates and adapting the clamping constraints to the base to the new distribution of the material.



Figure VI.XVI Smoothing process. Mesh before smoothing (left) and then (right).

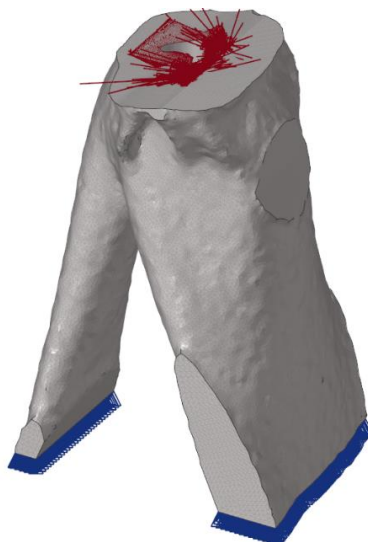


Figure VI.XVII FEA-Reanalysis of the new design space.

The mesh of the new design space was obtained following the smoothing process (opti-smoothing), which performs a better redistribution of the mesh elements as in Fig VI.XVI. The same reasoning is also applied to the second design space.

These optimized supports obtained are still too large. Certain of their optimal performance to support the component, they must however be reduced otherwise they would spend too much in terms of costs and time.

Therefore, it is necessary to optimize again one or more times, until the volume is the one desired and that the contact area is always supported: in fact, in this iteration phase, it is probable that the optimizer takes away material where the forces are of less intensity if you set optimization constraints on the fraction volume too low. In that case it is necessary to carry out reconstructions on the CAD modeling software, once the PARASOLID has been exported from Optistruct.

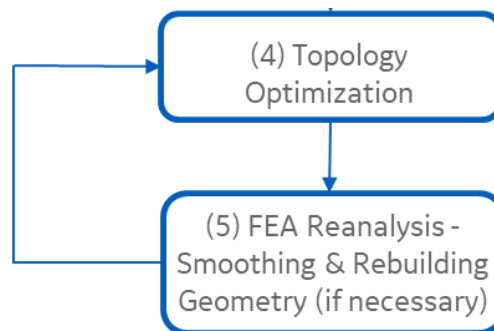


Figure VI.XVIII Detail of logic scheme: iteration process with topology optimization.

Model used

1stOptimized model of
Design Space I

Objective

Minimize Compliance

Optimization Constraint

UB Volume Fraction 0.4

Overhang 45°

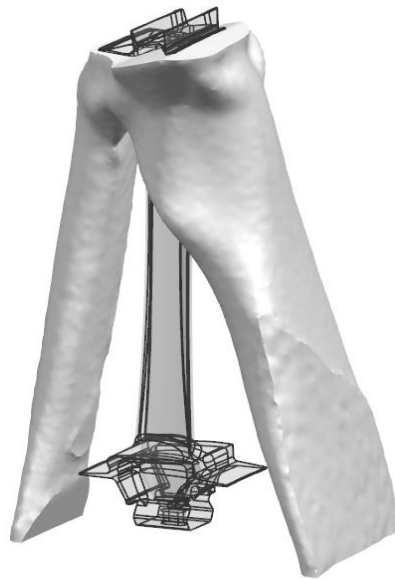


Figure VI.XIX Result of first iteration of Design Space I.

Volume	-60%
Compliance	+241,4%
Mass	-60%
Threshold	0.5
Iterations	46
Time	8h50

The percentage values correspond to an increase or decrease of the variable in consideration with respect to the optimized model of design space I. As expected, the computational cost has increased.

Model used	1 st Optimized model of Design Space II
Objective	Minimize Compliance
Optimization Constraint	UB Volume Fraction 0.45 Overhang 45°

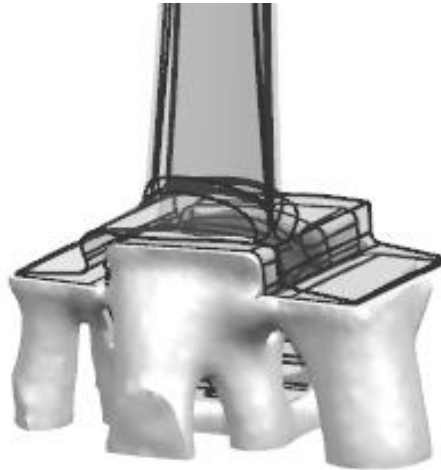


Figure VI.XX Result of first iteration of Design Space II.

Volume	-55%
Compliance	+109%
Mass	-55%
Threshold	0.5
Iterations	46
Time	2h5

The percentage values correspond to an increase or decrease of the variable in consideration with respect to the optimized model of design space II. This optimization is enough to efficiently support the overhang surfaces of angel wings, shank and dovetail. A further reduction in volume would lead to unsupported surfaces in overhang. As you can see, designing the widest design space II in one direction was effective for a good definition of load paths.

Model used

2nd Optimized model of
Design Space I

Objective

Minimize Compliance

Optimization Constraint

UB Volume Fraction 0.5

Overhang 45°

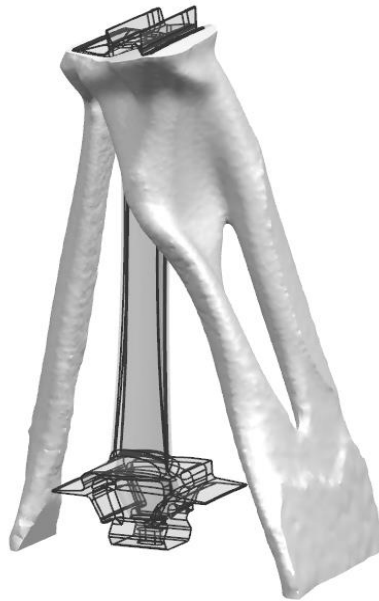


Figure VI.XXI Result of second iteration of Design Space I.

Volume	-50%
Compliance	209,2%
Mass	-50%
Threshold	0.6
Iterations	41
Time	15h56

This optimization is enough to efficiently support the overhang surfaces of shroud. A further reduction in volume would lead to unsupported surfaces in overhang.

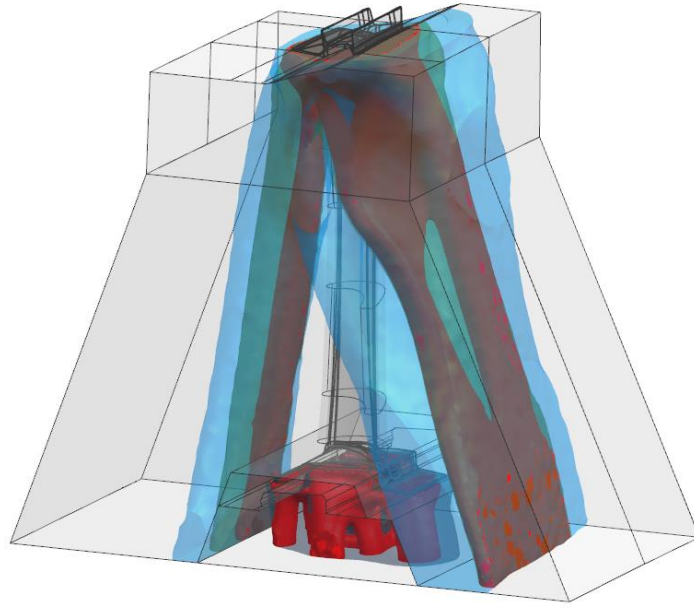


Figure VI.XXII Supports optimization iteration processes. In opaque gray the initial design spaces and in red color the final results. In opaque light blue the first optimization of the DS I, in opaque green second optimization of the DS I, in opaque midnight blue the first optimization of the DSII.

VI.VI. Validation of final support designs

As a last step, the generated method must be validated. To see the behavior during and after the printing process of the supported piece, the supports generated by the iterative topological optimization process are exported from Hypermesh as a .stl file. Then it is loaded together with the blade in the Additive simulation software and the thermo-mechanical analysis is performed again. To analyze the validity of the results, a comparison is made with the thermomechanical analysis of the same blade supported with traditional structures (Fig. VI.XXIII). From the analysis it can be seen that the deformations in the part of the shank, angel wings and dovetail are almost similar, with a slight improvement in the case of the optimized support. On the other hand, however, the maximum displacement on the shroud in the printing phase is about 20% higher: this, it is assumed, is due to a different stiffness distribution, since the lamellar structures have a total volume of material used 5% higher. The flexibility of this

methodology, therefore, allows to choose the volume fraction of the last iteration carried out slightly higher (for example 0.6), taking the same volume; this, with good probability, would lead to deformations that are certainly smaller and comparable to traditional supports, as the rigidity of the system will increase.

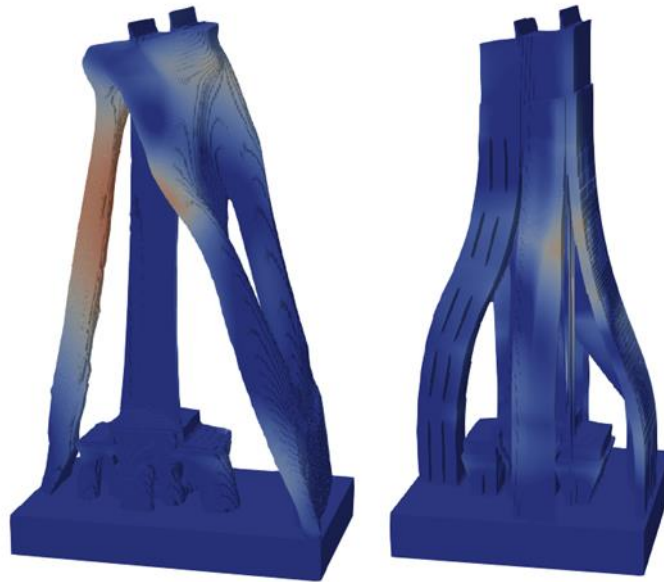


Figure VI.XXIII Thermomechanical analysis of the printing simulator. Deformation mapping: optimized support (left) and traditional support (right) with part.

An even greater advantage can be seen once the part is detached together with the supports from the platform, and then from the supports themselves. It can in fact be seen that, due to the high residual stresses concentrated in the blade when hold with lamellar supports, this deforms much more than the same with optimized supports.

In fact, it can be noted that in three extremes of the z shape of the shroud the deformations are definitely higher. In another extreme instead, the blade exhibits a better behavior: this is due to the fact that in the last iteration carried out, part of the material, and therefore part of stiffness, was subtracted from the optimizer, so that at that point the layer hasn't had the opportunity to spread heat to the support. In this case, a small correction of re-design of the support at this critical point would certainly have reduced the problem in question.

Moreover, even the side of the trailing edge of the foil closest to the shroud undergoes evident deformations: on average, with the optimized support, it is possible to obtain displacements of - 67%.

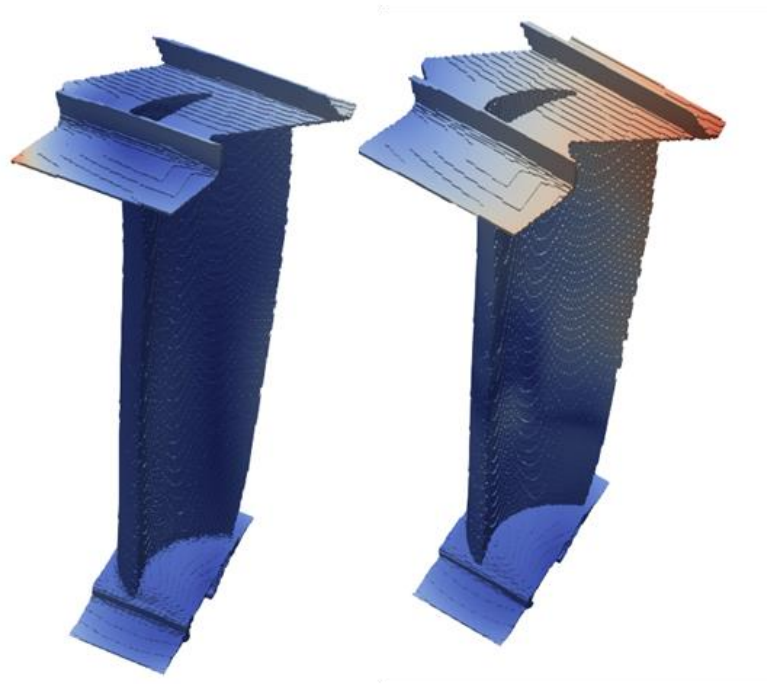


Figure VI.XXIV Blade after platform and supports removal at the end of printing process: blade previously supported by optimized structures (left) and by lamellar ones (right).

VII. Conclusions

Despite the good results obtained by the printing simulation, a real print is still needed to demonstrate the degree of reliability of the methodology. In this regard it is necessary to make some considerations. Since the contact area of these effective supports is practically the same and extended over the entire overhang surface, removal will be a factor that should not be underestimated, in particular if it concerns AM powder bed techniques with metallic materials. The progress achieved in generating this advanced methodology can however be exploited and adapted according to the needs. Several adaptations can be made.

One, for example, in which supporting structures can be generated by defining a volume of a certain quantity of thickness, between the overhang surfaces and the design space, which has a different density (or rather less) from that which the support itself actually has: in this way the presence of supports (such as the classic ones generated by Magics, teeth plus lamellar structures) is easily emulated. At the end of the iterative processes, the optimized interface volume is removed, and simple structures are inserted that have a smaller contact area (another example besides the classic ones are the lattice), so generating a hybrid support structure.

Another one may be the redesign, like in the final phases of the DFAM process explained in the third chapter, following the loading paths, "slicing" the reconstructed tubular solids and generating teeth that facilitate removal, so that the forces, applied by the component on the supports due to its deformation, continue to discharge where necessary.

Or simply, if you want to draw manually in a CAD environment, the deformations of the component, as seen in the initial part of the cycle (Fig. VI.VI and VI.VII), can be taken as input from which to start and then you can generate supporting structures to counterbalance.

So, in conclusion, thanks to the flexibility of this methodology, it can be taken into consideration in numerous applications to design support structures in future developments.

Appendix (A): L-Shaped geometry

The methodology was first tested on a L-shaped test component. A geometric form that allows you to create the problem in order to solve it. It has a vertical section that is self-sustained in contact with the build plate, and a horizontal section in complete overhang. [36]

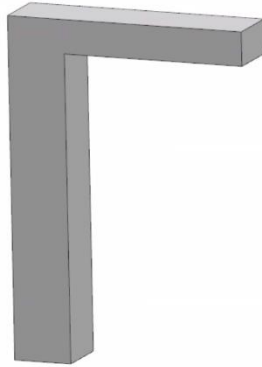


Figure A.I L-shaped geometry.

The methodology steps, for this test-case are illustrated below.

- **Mechanical and Thermal distortion model**

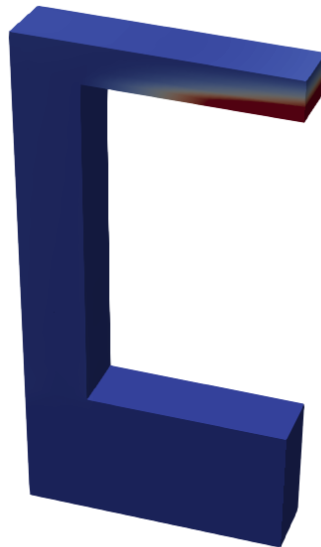


Figure A.II Distortion prediction of the L-shaped part.

- Preliminary support generation

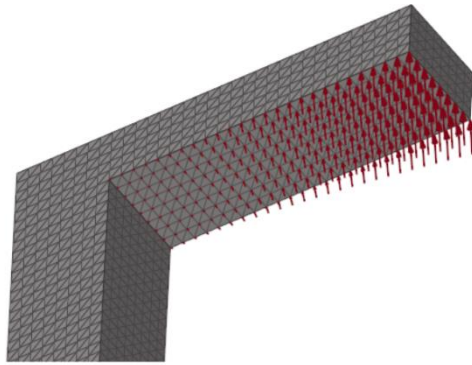


Figure A.III Displacement vectors interpolated to the FEM part.

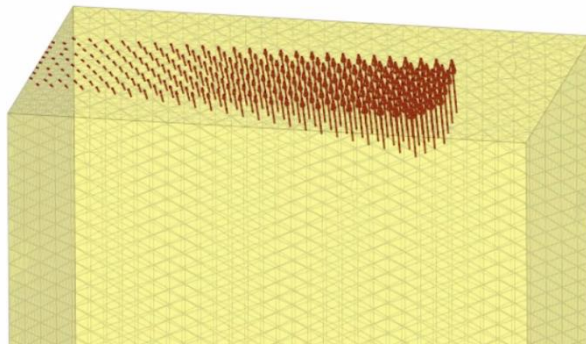


Figure A.IV Displacement vectors interpolated to the FEM of the preliminary support.

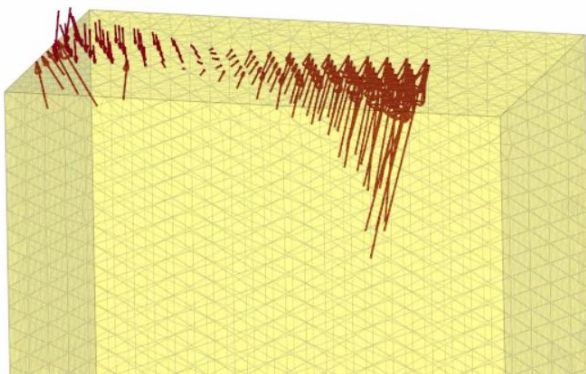


Figure A.V Force distribution, evaluated through static analysis.

- **Topology Optimization & Smoothing**

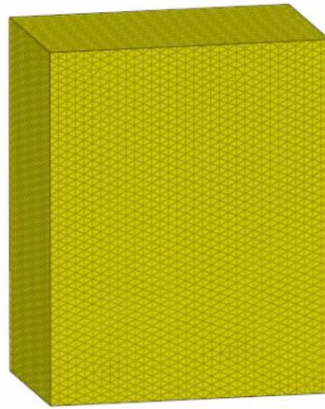


Figure A.VI Initial support Design Space.

OPTIMIZATION 1

<i>Objective</i>	<i>Min Compliance</i>
<i>Optimization Constraints</i>	<i>Volfracti 0.28</i>
	<i>Overhang 45°</i>
<i>Volume and Mass</i>	<i>-72%</i>

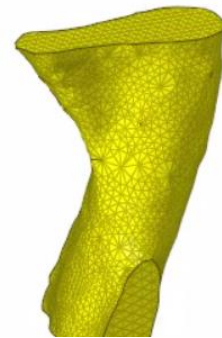


Figure A.VII Result Optimization 1.

OPTIMIZATION 2

<i>Objective</i>	<i>Min Compliance</i>
<i>Optimization Constraints</i>	<i>Volfracti 0.8</i>
	<i>Overhang 45°</i>
<i>Volume and Mass</i>	<i>-20%</i>

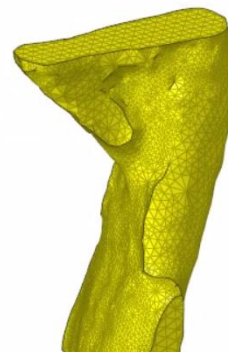


Figure A.VIII Result Optimization 2.

OPTIMIZATION 3

<i>Objective</i>	<i>Min Compliance</i>
<i>Optimization Constraints</i>	<i>Volfract 0.7</i>
	<i>Overhang 45°</i>
<i>Volume and Mass</i>	<i>-30%</i>

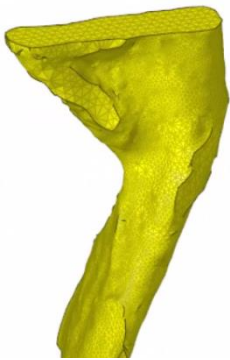


Figure A.IX Result Optimization 3.

- Final Support Design**

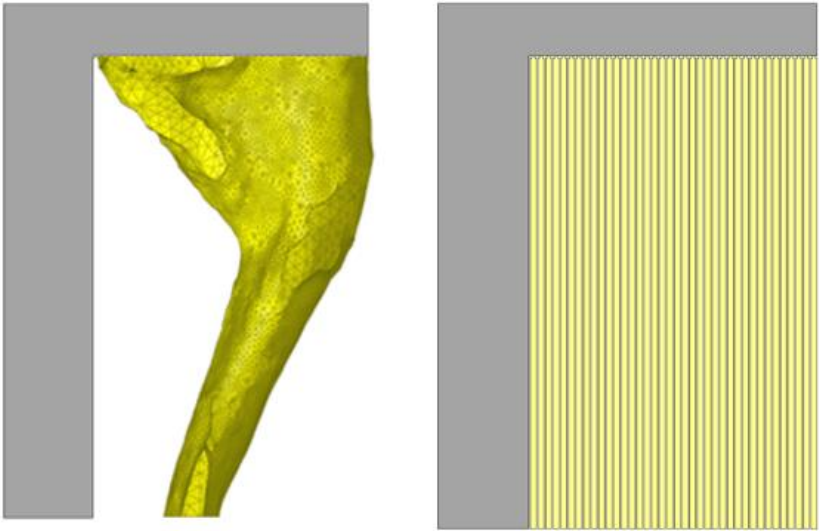


Figure A.X Final support design (left) and classical support (right).

- **Validation**

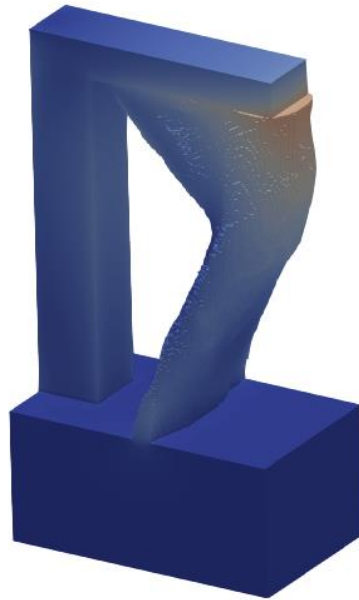


Figure A. XI Printing simulation of L-shaped with optimized support.

List of figures

FIGURE I.I CLASSIFICATION OF ADDITIVE MANUFACTURING TECHNIQUES.	5
FIGURE I.II ON THE LEFT SOME EXAMPLES OF EBM MELTING STRATEGY; ON THE RIGHT THE DIMENSIONS OF THE POWDERS USED FOR EBM AND SLM RESPECTIVELY.	6
FIGURE I.III EXAMPLE OF A DOE FULL FACTORIAL FOR EBM PROCESS WITH FOUR VARIABLES (BEAM SPEED, LINE OFFSET, POWER AND FOCUS OFFSET) ON TWO LEVELS (LOW/HIGH AND +/-): $2^4=16$ RUNS; HOW THEY INFLUENCE INTERNAL STRUCTURE OF SPECIMENS.	7
FIGURE I.IV DETAIL OF THE EBM SYSTEM.	8
FIGURE I.V POWDER BED METHODOLOGY OF AN EBM SYSTEM.	9
FIGURE I.VI ADVANTAGES (ON THE LEFT) AND DISADVANTAGES (ON THE RIGHT) OF PBF-EB.	10
FIGURE I.VII EOS EXPOSURE PROCESS IN THE SAME GAS DIRECTION (ON THE LEFT) AND OPPOSITE (ON THE RIGHT). ...	11
FIGURE I.VIII RESULTS BETWEEN DIFFERENT FUSION STRATEGIES IN THE SLM TECHNIQUE	11
FIGURE I.IX ADVANTAGES (ON THE LEFT) AND DISADVANTAGES (ON THE RIGHT) OF PBF-L.	12
FIGURE II.I EXAMPLE OF A STL MODEL STARTING FROM A CAD MODEL.	15
FIGURE II.II ACCEPTED ORIENTATION OF A CROSS SECTION.	17
FIGURE II.III EXAMPLE OF ADAPTIVE SLICING.	18
FIGURE II.IV STAIR-STEP EFFECT AND ITS REPRESENTATIONS IN THREE DIFFERENT AM TECHNOLOGIES.	18
FIGURE II.V PART EXTRACTION AFTER SLM PRINTING.	20
FIGURE III.I COST PER PART AS FUNCTION OF ITS COMPLEXITY.	22
FIGURE III.II COST PER PART AS FUNCTION OF NUMBER OF COMPONENTS TO BE BUILT.	22
FIGURE III.III ALL OPTIMIZATION CYCLE STARTING TO DESIGN SPACE DEFINITION TO VALIDATION OF NEW DESIGN AND PRINTING.	23
FIGURE III.IV EXAMPLE OF DESIGN SPACE AND NON-DESIGN SPACE.	25
FIGURE III.V SCHEME OF THE RE-ANALYSIS PROCESS OF AN OPTIMIZED COMPONENT.	28
FIGURE III.VI ISO-SURFACE AFTER TOPOLOGY OPTIMIZATION BEFORE (LEFT) AND LAPLACIAN SMOOTHING THEN (RIGHT).	29
FIGURE III.VII MESH BEFORE (LEFT) AND THEN (RIGHT) THE OPTI-SMOOTHING PROCESS.	30
FIGURE III.VIII EXAMPLE OF A RECONSTRUCTION OF A LOAD PATH CARRIED OUT THROUGH SURFACE EXTRUSIONS.	31
FIGURE III.IX EXAMPLE OF RECONSTRUCTION OF AN OPTIMIZED COMPONENT ON CATIA.	31
FIGURE IV.I KTT (KARUSH-KUHN-TUCKER) CONDITIONS FOR AN OPTIMIZATION PROBLEM. WITH GREY COLOR THE FEASIBLE REGION, AND x^* AS GLOBAL MINIMUM ON THE LEFT ($g \leq 0$ INACTIVE CONSTRAINT) AND AS LOCAL MINIMUM ON THE RIGHT	35
FIGURE IV.II OPTISTRUCT OPTIMIZATION METHODS FOR CONCEPT LEVEL DESIGN AND DESIGN FINE TUNING.	36
FIGURE IV.III CONTROL ARM TOPOLOGY OPTIMIZATION.	37
FIGURE IV.IV WORK SCHEME OF SIMP ALGORITHM FOR TOPOLOGY OPTIMIZATION.	39
FIGURE IV.V RELATIVE STIFFNESS IN FUNCTION OF DENSITY, VARYING PENALTY FACTOR.	39
FIGURE IV.VI EFFECT OF PENALTY FACTOR AND SENSITIVITY FILTER IN A 2D OPTIMIZATION PROBLEM.	40
FIGURE IV.VII EFFECT OF THE MESH ON THE OPTIMIZED STRUCTURE.	42
FIGURE IV.VIII EXAMPLES OF MICROSTRUCTURES WITH ROTATION: A) RECTANGULAR HOLES AND B) LAYERED	43
FIGURE IV.IX SHAPE OPTIMIZATION OF A CANTILEVER T-BEAM BEFORE (ON THE LEFT) AND THEN (ON THE RIGHT).	44
FIGURE IV.X TOPOGRAPHY OPTIMIZATION OF A L-BRACKET.	45
FIGURE IV.XI ON THE LEFT BEADS CREATED USING THE ELEMENT NORMAL METHOD; ON THE CENTRE BEADS CREATED USING THE USER DEFINED DRAW VECTOR METHOD; ON THE RIGHT THE SHAPE VARIABLES OF A BEAD.	46
FIGURE IV.XII DIRECTION TYPE ON OPTISTRUCT AVAILABLE FOR GRID POINTS.	47
FIGURE IV.XIII EFFECT OF TRANSITION ZONE DEFINITION ON FREE-SHAPE OPTIMIZATION.	47
FIGURE IV.XIV SHELL THICKNESS DISTRIBUTION BEFORE (ON THE LEFT) AND THEN (ON THE RIGHT) THE SIZE OPTIMIZATION.	48

FIGURE IV.XV SHELL CROSS-SECTION AND MINIMUM/MAXIMUM THICKNESS OF THE SHELL ELEMENT.	49
FIGURE IV.XVI FREE-SIZE OPTIMIZATION OF A WING RIB. RED ELEMENTS ARE UNCHANGED THICKNESS, BLUE ELEMENTS HAVE THICKNESS EQUAL TO 0.	49
FIGURE IV.XVII DIFFERENCE BETWEEN LOW, MEDIUM AND HIGH PRESENCE OF POROSITY AND THEIR INFLUENCE ON STIFFNESS PERFORMANCE (SEE EQUATION IV.V).	51
FIGURE IV.XVIII LATTICE STRUCTURAL OPTIMIZATION OF A CONTROL ARM WITH TETRAHEDRAL ELEMENTS.	51
FIGURE V.I NUMBER OF PUBLISHED PAPERS FOR AM AND SUPPORT STRUCTURES.	52
FIGURE V.II A) STRESS GRADIENT DURING MELTING AND STRESS RESIDUAL AFTER COOLING; B) SUPPORT STRUCTURES (GREEN) FOR PRINTABILITY; C) SUPPORT STRUCTURES FOR BALANCE.	53
FIGURE V.III METHODS TO REDUCE THE PRESENCE OF SUPPORTS.	55
FIGURE V.IV TEETH OF A SUPPORT STRUCTURE AND ITS CHARACTERISTICS.	56
FIGURE V.V EXAMPLES OF DIFFERENT TYPES OF SUPPORT STRUCTURES.	56
FIGURE V.VI CONSIDERATION FOR SUPPORT STRUCTURE DESIGN.	57
FIGURE V.VII(A) SUPPORTED AND UNSUPPORTED OVERHANG FEATURES AT A CRITICAL ANGLE θ AND (B) WARPING PRINCIPLE IN THE SECOND ONE: THE EFFECTIVE INCLINED ANGLE θ' BETWEEN THE OVERHANGING PART OF THE LAYER AND THE PREVIOUS LAYER IS SMALLER THAN THE DESIGNED INCLINED CRITICAL ANGLE θ	58
FIGURE V.VIII A SIMPLE PART BUILT WITH SUPPORTS ON THE LEFT. THE SAME PART WITHOUT ANY SUPPORT ON THE RIGHT (LITTLE SUPPORT ONLY FOR EDM) BUILT AT 45°	59
FIGURE V.IX SCHEMATIC OF FIRST STEP OPTIMIZATION FOR OPTIMAL ORIENTATION TO REDUCE SUPPORT VOLUME	59
FIGURE V.X FROM THE LEFT, GYROID AND DIAMOND LATTICE STRUCTURES IN A 4x4 CELL.	61
FIGURE V.XI EXAMPLE HOW UNIT CELLS VOXELS GENERATE A SUPPORT STRUCTURE.	61
FIGURE V.XII A) "IY" SUPPORT STRUCTURE FOR A THIN PLATE; B) "Y" SUPPORT STRUCTURE; C) ARRAY OF PINS SUPPORT STRUCTURES.	62
FIGURE V.XIII A GENERAL WORKFLOW TO EXECUTE A TO FOR SUPPORT STRUCTURES.	63
FIGURE VI.I LOW-PRESSURE TURBINE BLADE TO BE PRINTED; 1) FINS 2) SHROUD 3) FOIL OR BLADE BODY 4) ANGEL WINGS 5) SHANK 6) FIR TREE OR DOVETAIL.	65
FIGURE VI.II LOGICAL SCHEME TO EXECUTE TOPOLOGY OPTIMIZATION FOR SUPPORTS.	65
FIGURE VI.III INDIVIDUATION OF OVERHANG SURFACES (COLOR: RED). THESE SURFACES WILL REPRESENT THE AREAS OF CONTACT BETWEEN THE PART AND THE SUPPORT.	66
FIGURE VI.IV ANCHOR VOLUME WITH LOW MECHANICAL PROPERTY AND LOW DENSITY AS SUPPORT INTO RED CIRCLE. IN THE CENTRE THE BLADE WITH ANCHORAGE (RED). ON THE RIGHT THE SIMULATION AND MAGNITUDE DISPLACEMENTS MAPPING.	68
FIGURE VI.V DETAIL OF A SAME MESHED SURFACE ON SIMULATOR SOFTWARE (QUAD ON THE LEFT) AND HYPERMESH (R-TRIA ON THE RIGHT)	69
FIGURE VI.VI DISPLACEMENTS MAPPING ON THE SHROUD SURFACES.	69
FIGURE VI.VII DISPLACEMENTS MAPPING ON ANGEL WINGS, SHANK AND DOVETAIL.	70
FIGURE VI.VIII DESIGN SPACE GENERATION ON THE TOP (RIGHT) AND BOTTOM (LEFT) OF THE TURBINE BLADE.	70
FIGURE VI.IX DESIGN SPACES ON THE PLATFORM OF AM MACHINE.	71
FIGURE VI.X DETAIL OF CONSTRAINT UNDER THE BASE OF THE PRELIMINARY SUPPORT OF THE SHROUD.	72
FIGURE VI.XI DISPLACEMENTS AS VECTOR FORM (LEFT) AND AS CONSTRAINT (RIGHT) OF THE PRELIMINARY SUPPORT OF THE SHROUD.	72
FIGURE VI.XII FORCE DISTRIBUTION ON THE PRELIMINARY SUPPORT FOR THE SHROUD.	73
FIGURE VI.XIII FORCE DISTRIBUTION ON THE PRELIMINARY SUPPORT FOR ANGEL WINGS, DOVETAIL AND SHANK.	73
FIGURE VI.XIV RESULT OF FIRST OPTIMIZATION FOR DESIGN SPACE I.	74
FIGURE VI.XV RESULT OF FIRST OPTIMIZATION FOR DESIGN SPACE II.	76
FIGURE VI.XVI SMOOTHING PROCESS. MESH BEFORE SMOOTHING (LEFT) AND THEN (RIGHT).	77
FIGURE VI.XVII FEA-REANALYSIS OF THE NEW DESIGN SPACE.	77
FIGURE VI.XVIII DETAIL OF LOGIC SCHEME: ITERATION PROCESS WITH TOPOLOGY OPTIMIZATION.	78
FIGURE VI.XIX RESULT OF FIRST ITERATION OF DESIGN SPACE I.	79

FIGURE VI.XX RESULT OF FIRST ITERATION OF DESIGN SPACE II.	80
FIGURE VI.XXI RESULT OF SECOND ITERATION OF DESIGN SPACE I.....	81
FIGURE VI.XXII SUPPORTS OPTIMIZATION ITERATION PROCESSES. IN OPAQUE GRAY THE INITIAL DESIGN SPACES AND IN RED COLOR THE FINAL RESULTS. IN OPAQUE LIGHT BLUE THE FIRST OPTIMIZATION OF THE DS I, IN OPAQUE GREEN SECOND OPTIMIZATION OF THE DS I, IN OPAQUE MIDNIGHT BLUE THE FIRST OPTIMIZATION OF THE DSII.	82
FIGURE VI.XXIII THERMOMECHANICAL ANALYSIS OF THE PRINTING SIMULATOR. DEFORMATION MAPPING: OPTIMIZED SUPPORT (LEFT) AND TRADITIONAL SUPPORT (RIGHT) WITH PART.	83
FIGURE VI.XXIV BLADE AFTER PLATFORM AND SUPPORTS REMOVAL AT THE END OF PRINTING PROCESS: BLADE PREVIOUSLY SUPPORTED BY OPTIMIZED STRUCTURES (LEFT) AND BY LAMELLAR ONES (RIGHT).....	84

FIGURE A.I L-SHAPED GEOMETRY.....	87
FIGURE A.II DISTORTION PREDICTION OF THE L-SHAPED PART.....	87
FIGURE A.III DISPLACEMENT VECTORS INTERPOLATED TO THE FEM PART.	88
FIGURE A.IV DISPLACEMENT VECTORS INTERPOLATED TO THE FEM OF THE PRELIMINARY SUPPORT.	88
FIGURE A.V FORCE DISTRIBUTION, EVALUATED THROUGH STATIC ANALYSIS.....	88
FIGURE A.VI INITIAL SUPPORT DESIGN SPACE.	89
FIGURE A.VII RESULT OPTIMIZATION 1.	89
FIGURE A.VIII RESULT OPTIMIZATION 2.	89
FIGURE A.IX RESULT OPTIMIZATION 3.....	90
FIGURE A.X FINAL SUPPORT DESIGN (LEFT) AND CLASSICAL SUPPORT (RIGHT).	90
FIGURE A. XI PRINTING SIMULATION OF L-SHAPED WITH OPTIMIZED SUPPORT.	91

List of tables

TABLE I.I GENERAL TECHNICAL FEATURES COMPARED BETWEEN THE TWO TECHNOLOGIES, EBM AND SLM.	13
TABLE III.I RESPONSES IN OPTISTRUCT SOFTWARE	26
TABLE IV.I DEFAULT DISCRETE AND PENALTY VALUES FOR TOPOLOGY OPTIMIZATION	41
TABLE V.I SOME OF AM TECHNOLOGIES AND NEED OF SUPPORT STRUCTURES.	54

Bibliography

- [1] International Committee F42 for Additive Manufacturing Technologies, ASTM.
- [2] Ian Gibson, David W. Rosen, Brent Stucker, *Additive Manufacturing Technologies, Rapid Prototyping to Direct Digital Manufacturing*, Springer.
- [3] Chee Kai Chua, Kah Fai Leong, *3D Printing and Additive Manufacturing*.
- [4] Gaytan SM, Murr LE, Medina F, Martinez E, Lopez MI, Wicker RB (2009) *Advanced metal powder-based manufacturing of complex components by electron beam melting*.
- [5] Murr LE, Gaytan SM, Medina F, Lopez H, Martinez E, Machado BI, Hernandez DH et al (2010) *Next-generation biomedical implants using additive manufacturing of complex, cellular and functional mesh arrays*.
- [6] Murr LE, Martinez E, Gaytan SM, Ramirez DA, Machado BI, Shindo PW, Martinez JL et al (2011) *Microstructural architecture, microstructures, and mechanical properties for a nickel-base superalloy fabricated by electron beam melting*.
- [7] Baufeld B, Brandl E, van der Biest O (2011) *Wire based additive layer manufacturing: comparison of microstructure and mechanical properties of Ti–6Al–4V components fabricated by laser-beam deposition and shaped metal deposition*.
- [8] John O.Milewski, *Additive Manufacturing of Metals*, Springer (2017)
- [9] Ian Gibson, David Rosen, Brent Stucker, *Additive Manufacturing Technologies*, Springer (2015)
- [10] Department of Management and Production Engineering, *Design guidelines for Direct Metal Laser Sintering (DMLS)*, Politecnico di Torino (2018).
- [11] B. Vayre, F. Vignat, F. Villeneuve, *Designing for Additive Manufacturing*, Elsevier (2012)
- [12] *Hyperworks 14.0, Optistruct Tutorials and Examples*, Altair.
- [13] G. Strang and G. Fix, *An analysis of the finite element method*, Wellesley Cambridge Press, Wellesley, MA, second ed., 2008.
- [14] W. R. Buell and B. A. Bush, *Mesh generation -a survey*, J. Manuf. Sci.Eng., 1973.
- [15] Eynard, B., Nigrelli, V., Oliveri, S.M., Peris-Fajarnes, G., Rizzuti, S. *Advances on Mechanics, Design Engineering and Manufacturing: Proceedings of the*

International Joint Conference on Mechanics, Design Engineering & Advanced Manufacturing (JCM 2016), 2016, Catania, Italy.

[16] Anton Olason, Daniel Tidman “*Methodology for Topology and Shape Optimization in the Design Process*”.

[17] Altair HyperWorks, <https://altairhyperworks.com/solution/Optimization>.

[18] Wikipedia, <https://en.wikipedia.org/wiki/Topology>

[19] M.P. Bendsøe and O. Sigmund. *Topology Optimization; Theory, Methods and Applications*. Springer, 2th edition, 2004.

[20] Mohammad Rouhi. *Topology optimization of continuum structures using element exchange method*. Master's thesis, Mississippi State University, 2009.

[21] M. Stolpe and K. Svanberg. *An alternative interpolation scheme for minimum compliance topology optimization*. Structural Multidisciplinary Optimization, 2001.

[22] P.M. Clausen O. Sigmund. *Topology optimization using a mixed formulation: An alternative way to solve pressure load problems*. Computer Methods in Applied Mechanics and Engineering, 2006.

[23] Martin Philip Bendsøe and O. Sigmund. *Material interpolation schemes in topology optimization*. Archive of Applied Mechanics, 1999.

[24] Hans A. Eschenauer and Niels Olhoff. *Topology optimization of continuum structures: A review*. Appl. Mech. Rev, 2001.

[25] Martin Philip Bendsøe and Noboru Kikuchi. *Generating optimal topologies in structural design using a homogenization method*. Computer Methods in Applied Mechanics and Engineering, 1988.

[26] Marco Cavazzuti, *Introduzione alle tecniche di ottimizzazione*, Università degli Studi di Modena e Reggio Emilia, 2013.

[27] Jingchao Jiang , Xun Xu and Jonathan Stringer, *Support Structures for Additive Manufacturing: A review*, *Journal Of Manufacturing and materials processing*, 2018.

[28] Ly Yang, Keng Hsu, Brian Baughman, Donald Godfrey, Francisco Medina, Mamballykalathil Menon, Soeren Wiener, *Additive Manufacturing of metals: The technology, Materials, Design and Production*, Springer, 2017

[29] Thrimurthulu, K.P.P.M.; Pandey, P.M.; Reddy, N.V. *Optimum part deposition orientation in fused deposition modeling*. Int. J. Mach. Tools Manuf. 2004.

- [30] F. Calignano, Elsevier, *Design optimization of supports for overhanging structures in aluminum and titanium alloys by selective laser melting*, Materials and Design, 2014.
- [31] Hildreth, O.J.; Nassar, A.R.; Chasse, K.R.; Simpson, T.W. *Dissolvable Metal Supports for 3D Direct Metal Printing*. *3D Print. Addit. Manuf.* 2016
- [32] Hussein, A.; Hao, L.; Yan, C.; Everson, R.; Young, P. *Advanced lattice support structures for metal additive manufacturing*. *J. Mater. Process. Technol.* 2013.
- [33] Vaidya, R.; Anand, S. *Optimum Support Structure Generation for Additive Manufacturing Using Unit Cell Structures and Support Removal Constraint*. *Procedia Manuf.* 2016
- [34] Gan, M.X.; Wong, C.H. *Practical support structures for selective laser melting*. *J. Mater. Process. Technol.* 2016.
- [35] Francesco Mezzadri, Vladimir Bouriakov, Xiaoping Qian, *Topology optimization of self-supporting support structures for additive manufacturing*, Elsevier, 2018.
- [36] Luciano Coniglio, *Methods for improved build feasibility in Additive Manufacturing*, Master Thesis, Politecnico di Torino, 2019

